9-2007

# Conceptual MEMS Devices for a Redeployable Antenna

Virginia Miller


# CONCEPTUAL MEMS DEVICES FOR A REDEPLOYABLE ANTENNA

THESIS

Virginia Miller, Second Lieutenant, USAF

AFIT/GE/ENG/07-30

**DEPARTMENT OF THE AIR FORCE**
**AIR UNIVERSITY**

***AIR FORCE INSTITUTE OF TECHNOLOGY***

**Wright-Patterson Air Force Base, Ohio**

The views expressed in this thesis are those of the author and do not reflect the official policy or position of the United States Air Force, Department of Defense, or the U.S. Government.

AFIT/GE/ENG/07-30

# CONCEPTUAL MEMS DEVICES FOR A REDEPLOYABLE ANTENNA

THESIS

Presented to the Faculty

Department of Electrical and Computer Engineering

Graduate School of Engineering and Management

Air Force Institute of Technology

Air University

Air Education and Training Command

In Partial Fulfillment of the Requirements for the

Degree of Master of Science in Electrical Engineering

Virginia Miller, BS

Second Lieutenant, USAF

September 2007

AFIT/GE/ENG/07-30

# CONCEPTUAL MEMS DEVICES FOR A REDEPLOYABLE ANTENNA

Virginia Miller, BS

Second Lieutenant, USAF

Approved:

| | |
|---|---|
| _____\\signed_____ | 31 Aug 07 |
| LaVern A. Starman, Maj, USAF (Chairman) | Date |
| _____\\signed_____ | 31 Aug 07 |
| James A. Fellows, Lt Col, USAF (Member) | Date |
| _____\\signed_____ | 31 Aug 07 |
| Ronald A. Coutu, Jr., Maj, USAF (Member) | Date |

## Abstract

Micro-Electro-Mechanical Systems (MEMS) are becoming an integral part of our lives through a wide range of applications, including MEMS accelerators for air bag deployment in vehicles, micromirrors in projection devices, and various sensors for chemical/biological applications. MEMS are a key aspect of ever-increasing significance in a myriad of commercial and military applications. Because of this importance, this thesis utilizes MEMS devices that can deploy and retract an antenna suitably sized for placement on an insect or microrobot for communication purposes. A target monopole antenna with a length of 1 mm was used as a test metric. From this requirement, several MEMS designs using scratch drives and thermal actuators as the basis for powering the motor were developed. Some of the fabricated and tested designs included a gear with side flaps that flip up perpendicular to the substrate; gears that push an antenna beam off the edge of the substrate; and an antenna beam that is moved upwards such that it stands perpendicular to the substrate. These designs had the highest likelihood of success. Other designs included an array of micro gears and guiding beams, a large wheel powered by scratch drives, and a gear with the pawl requiring assembly. For these designs to be successful, several basic modifications would be necessary. The antenna beam that moves into a position perpendicular to the substrate was successfully self-assembled.

**Acknowledgments**

Many thanks are due to Maj. Starman for all his instruction about testing, designs, and MEMS in general; for listening to and commenting on my ideas; for giving me suggestions with which to work; and for his many revisions of this document. Maj. Kading is also deserving of my gratitude, as he was extremely helpful with envisioning and creating designs as well as testing them. Capt. Allard, Capt. Bellott, and Capt. Glauvitz, who all endured my incessant questioning my first two quarters, are also deserving of my gratitude. Finally, I would like to thank all those folks in my MEMS classes for tolerating the piecemeal learning so that I would receive the information I needed before this work was due.

Virginia Miller

## Table of Contents

Page

## List of Figures

Page

## List of Tables

Page

# CONCEPTUAL MEMS DEVICES FOR A REDEPLOYABLE ANTENNA

## I. Introduction

### Problem Statement

In both the commercial and military arenas, microelectromechanical systems (MEMS) are becoming more widespread then ever before and their potential applications are nearly endless. Because of the small, sub-millimeter size of MEMS structures, these devices are of vital importance to a new military focus by the Defense Advanced Research Projects Agency (DARPA) in the integration of MEMS with insects, known as the Hybrid Insect MEMS (HI-MEMs) program. Outside of the power requirements necessary for device operation, a key element of the HI-MEMs project is enabling communication not only with the insect but also with the MEMS integrated system. From this requirement, the purpose of this thesis is drawn: detail the design of a MEMS device to deploy and retract an antenna that is capable of being used as a communication device in an insect or a microrobot in order to facilitate communication between an insect or microrobot and its controller.

### Research Objective

The objective of this research is to investigate a variety of MEMS devices that can potentially be used to retract and deploy an antenna. This investigation includes the design, fabrication and subsequent testing of the MEMS devices as well as determining the feasibility of the designed device in an operational condition. The process followed

throughout this research involves identifying several possible designs that have the greatest potential to be successfully utilized in a microrobot or insect. An ideal solution would enable the antenna to be repeatedly deployed and retracted in a rapid manner to prevent any potential damage from the flight of the insect or microrobot.

**Research Focus**

The timeline for this research is somewhat restricted, thereby limiting it to several proof-of-concept retractable antenna designs. The primary focus involves identifying devices that operate without an attached antenna or that have a polysilicon beam as a substitute antenna such that the actual antenna itself could be added later in a post-processing step. Scratch drives and electrothermal actuators are investigated for their mechanical forces exerted on a MEMS gear, while hinges, locks, solder balls, and residual stress cantilevers comprise the functional aspects of several different devices.

**Preview**

The remainder of this thesis is divided into four chapters. Chapter II describes in detail the background associated with the selected devices, the Multi-User MEMS Process (MUMPs) fabrication technology, and various hinge mechanisms. Chapter III explains the methodology used to design the MEMS devices, as well as a description of each developed device. Chapter IV covers the numerical analysis, as well as testing methodology and the corresponding results and analysis, performed on the fabricated devices. Lastly, Chapter V provides the conclusions of this research and future

recommendations to further develop and enhance the designed devices along with ideas for other MEMS structures able to retract and deploy an antenna.

# II. Background

## Chapter Overview

This chapter discusses the purposes and applications of a retractable antenna, as well as an overview of the PolyMUMPs fabrication process utilized in the antenna design. As technology continues to shrink, the ability of using microstructures for reconnaissance becomes more of a reality. In developing a retractable antenna, a variety of microstructures are used to achieve the desired end product. Locomotion sources include scratch drives and thermal actuators, while hinges, solder balls, locking mechanisms, and residual stress beams play key roles in several of the antenna designs.

## Relevant Research

The following section gives background information on the DARPA-funded HI-MEMS project and other MEMS-based microrobots and their power sources. Additionally, this section covers previously developed MEMS antennas and briefly addresses the PolyMUMPs fabrication process.

### *Hybrid-insect MEMS*

Researchers have been using flying insects as models to develop small flying robots, as flight of insects has been controlled using electrical muscle stimulation [3]. Consequently, DARPA wants to investigate using flying insects directly in research concerning HI-MEMS for several reasons [15]. Insects already know how to fly, have natural camouflage, are robust, are present in nearly all environments across the globe, and can easily adapt to their surroundings. Furthermore, creating a myriad of such

cyborgs can be done at a low cost since a robotic platform does not need to be built. Such insects could be used for carrying payloads between 0.5 and 5 grams. MEMS can provide key components to control insect motion and harness power from the insect by using the creatures' muscles to garner mechanical energy, and collecting thermal energy from body and muscle heat [16]. The mechanical and thermal energies gathered can then be used to generate electrical energy. A moth's muscles output approximately 1 W of power. Converting 10% of that muscle power to mechanical energy can yield 1 mW without affecting the flight of the insect, or 10 mW if the insect is not airborne. The thermal energy from those muscles, assuming 0.25% efficiency, can yield approximately 2.7 mW of electrical energy [16].

The flying insects are being studied the most since they can travel rapidly over long distances, although insects that swim or hop are also being investigated. Monarch butterflies could be useful in long-distance missions for example, since they can go without food for 75 days and travel 3000 miles. The white witch moth (*Thysania agrippina*) could be used for carrying relatively large payloads, as it has a wingspan of 25 cm, the largest of the Lepidoptera order [16]. Dragonflies, which can travel at speeds around 45 mph, could be utilized for missions where time is of the essence. Due to the small size of MEMS devices, most insects could serve as viable transportation for an on board system.

By placing a chip inside an insect still in the metamorphic stage, the insect's tissue will grow to completely encompass the device as if it were a natural part of the insect. Such implants have been shown to be completely integrated in the insect's body,

as shown in Figure 1 [20]. In order to control the motion of the insect, an implanted device can emit ultrasonic pulses, use pheromones, distort the image of what the insect sees, or even use electrical pulses to control the muscles [16].

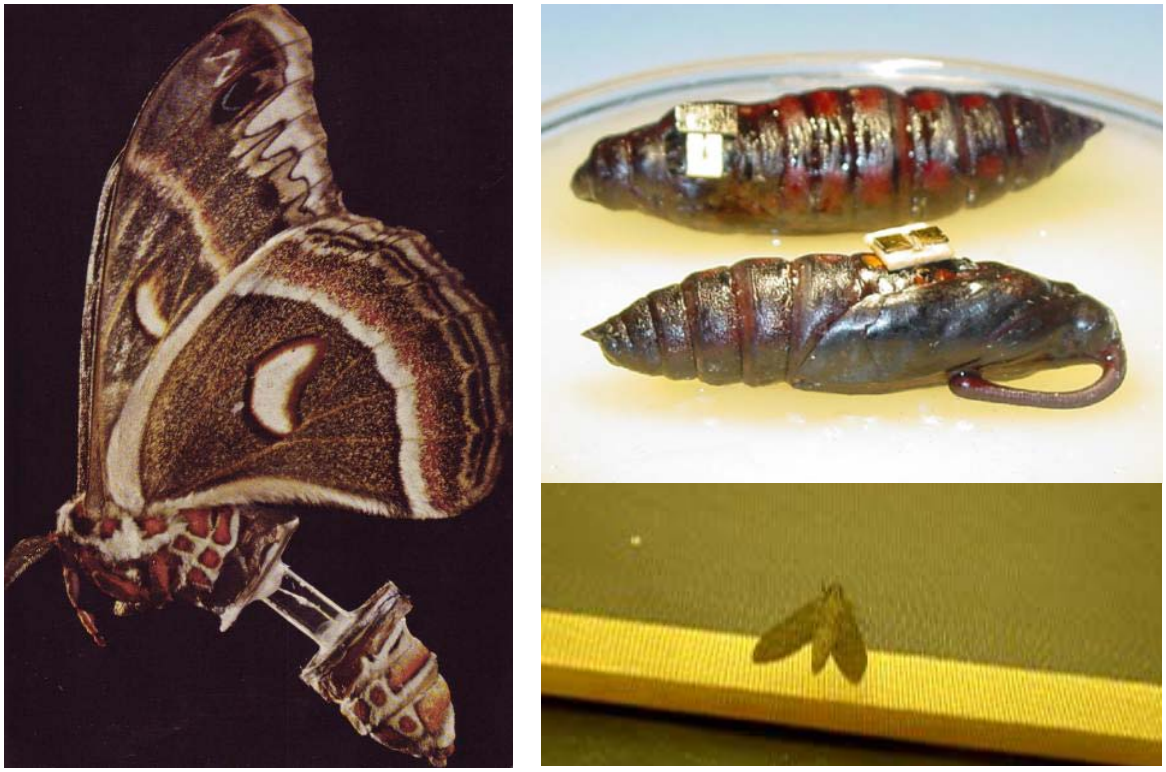

**Figure 1: Photo of moth with pipe inserted in pupa stage (left) for hormone transport and moth with balsa platform (right) stitched into pupae stage [16].**

To counteract the natural tendencies of insects to feed, reproduce, and respond to changes in the environment, either MEMS devices or genetic manipulation can be used. The latter would likely require a great deal of time to become a useful technology; therefore, MEMS are the potential devices that are being researched at DARPA.

***Microrobots***

As unmanned aerial vehicles (UAVs), microrobots are appealing for military applications due to their small size and relative unobtrusiveness. However, one important

problem plaguing the research and use of microrobot is the lack of a micro power source [15]. Creating an energy source that can supply a great deal of power while having a low mass density has been an impediment to the development of such UAVs. One group of researchers has created a micro photosynthetic electrochemical cell that uses metabolic processes from the blue-green algae *Anabaena.* In this cell, respiration and photosynthesis create electrical energy without needing fuel, and the former process creates energy in both light and dark conditions [18]. Other scientists have developed a solar cell using photosystems from spinach, but it is not currently feasible for use in powering a UAV [17].

An untethered robot has been developed that can move because of an applied voltage to the substrate on which it rests. Shown in Figure 2, it is a simple design, comprised only of a scratch drive and a steering beam and it can be directed relatively easily. Four possible configurations exist for this robot: the arm can be either in the up or down position, and the scratch drive actuator can be bent or straight. The different positions of the scratch drive cause the robot to move, while the positions of the arm control its turning ability [8]. A different method for powering a microrobot involves vibrating the ground at a particular frequency; if that frequency is the same as the natural frequency of the insect-like robot's leg, then the robot will move [19]. Another group of researchers used a photo-thermo-mechanical actuation system to power microrobotic legs. A light shines on a thermal actuator, causing a cantilever to bend similar to the bending of an insect's leg [2].

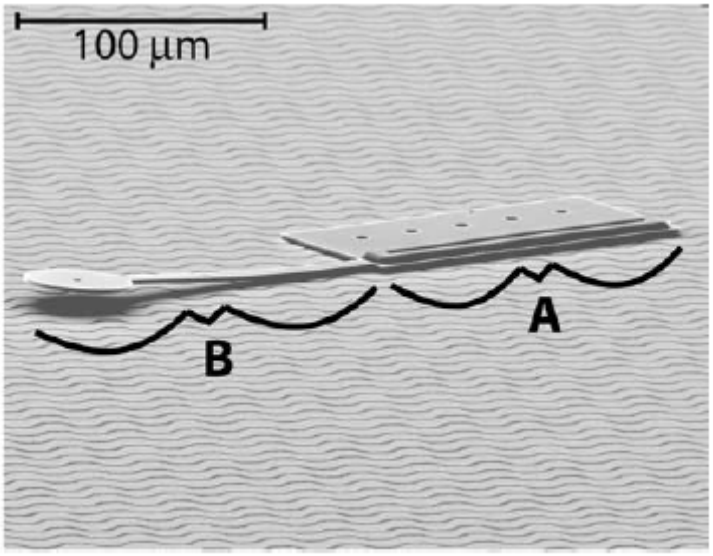


**Figure 2: Untethered robot with scratch drive (A) and steering arm (B) [8].**

***Antennas***

MEMS technology has previously been used with antennas; one group of researchers developed a reconfigurable Vee-antenna whose arms are moved by independently controlled microactuators, as depicted in Figure 3. This antenna, however, was designed for use at 17.5 GHz [6].

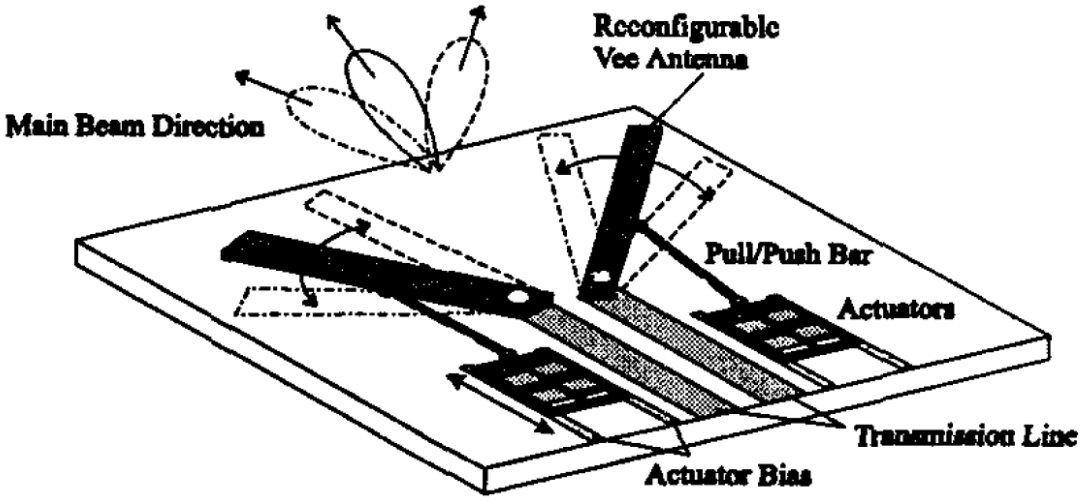


**Figure 3: Reconfigurable Vee-antenna with actuator controls [6].**

Another group of researchers integrated an antenna with RF MEMS switches, but its size of several millimeters makes it too large for use in this project [5]. Researchers at Georgia Tech have created several types of antennas, among them a fixed 800 µm vertical antenna that resonated at 85 GHz and a W-band Yagi-Uda antenna that resonated at 100 GHz, shown in Figure 4 [29, 30]. They have also created a patch antenna that is elevated off the substrate that operates in the 20-30 GHz range [32].

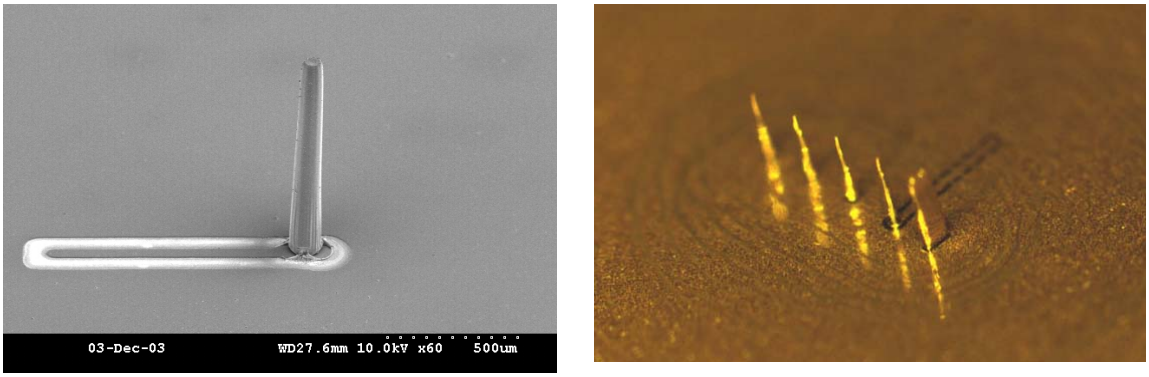


**Figure 4: Fixed 800µm antenna (right) [30] and W-band vertical Yagi-Uda antenna (left) [31].**

***PolyMUMPs Fabrication Process***

The PolyMUMPs component of the MUMPs program was used for fabrication of the proof-of-concept designs in this research. PolyMUMPs has a minimum feature size of 2 µm and is comprised of three polysilicon layers, two sacrificial layers, and one metal layer as shown in Figure 5.

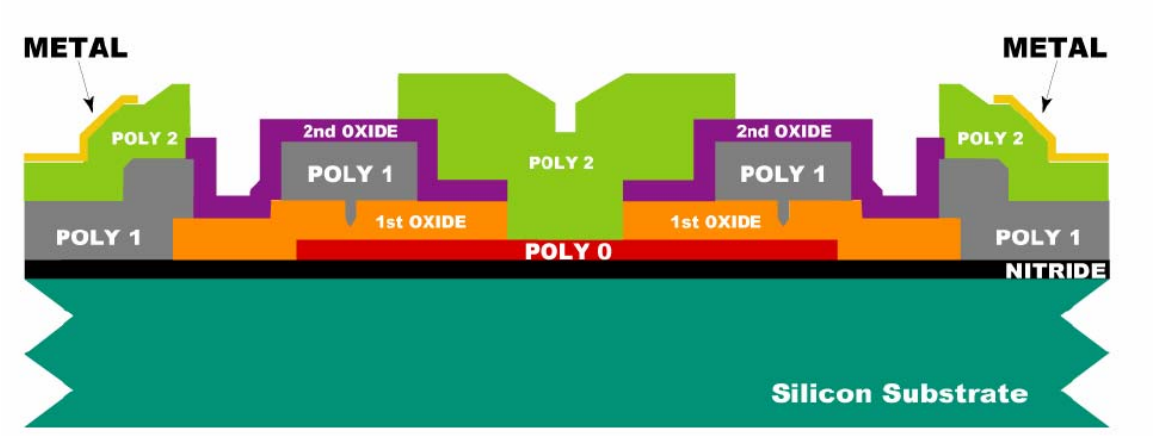


**Figure 5: PolyMUMPs fabrication layers [21].**

An n-type (100) silicon wafer is doped with phosphorous via a dopant source of a phosphosilicate glass (PSG) sacrificial layer. A 600 nm electrically isolating layer of silicon nitride is then deposited by means of low pressure chemical vapor deposition (LPCVD). The first polysilicon layer, Poly0, is deposited by LPCVD and patterned via photolithography. This process involves covering the wafer with photoresist, exposing the wafer to UV radiation through a mask, and then developing the photoresist to create a pattern for etching. This method of patterning is used on each of the subsequent layers. The Poly0 layer is then etched via a reactive ion etch (RIE) and the photoresist is removed. Another layer of PSG, known as the first oxide, is then deposited and annealed. This 2 μm thick sacrificial layer is removed at the end of the process to free the first releasable layer, Poly1. The first oxide layer is lithographically patterned with a DIMPLE mask and undergoes an RIE, which results in dimples that are 750 nm deep. The oxide is then patterned once more with an ANCHOR1 mask and RIE to enable the Poly1 layer to attach to the Poly0 or the nitride layer.

Poly1, the second polysilicon layer of 2 μm, is then deposited. A 200 nm layer of PSG is deposited on top and then the wafer is annealed to dope the Poly1 layer with phosphorous from the PSG from both the top and the bottom, after which the layer is again patterned via RIE. A second 0.75 μm sacrificial layer of PSG is then deposited. This layer is patterned and etched with the POLY1_POLY2_VIA mask, removing the second oxide so the Poly2 layer can be physically attached to the Poly1 layer. An ANCHOR2 layer is patterned and etched in the same manner; however, this etch removes both the first and second oxide layers such that the Poly2 layer can be anchored to the Poly0 or nitride layer.

A third 1.5 μm thick polysilicon layer known as Poly2 is then deposited. Again, as with the Poly1, a 200 nm PSG mask is deposited and annealed to dope the Poly2 to reduce residual stress and increase conductivity. The Poly2 layer is then patterned and etched. The final layer is gold and is evaporated on with a 0.5 μm thickness. It is patterned via a metal lift-off technique. The gold layer only adheres to the Poly2 layer.

Once the chip has been fabricated and returned, it is immersed in acetone to remove the protective layer of photoresist. The chip is then placed in hydrofluoric acid to remove the sacrificial oxide layers, thereby freeing structures to move. Drying of the chip can take place either in a $CO_2$ dryer or on a hotplate. For the former drying method, the chip is removed from the HF and placed into a methanol solution before being placed in the dryer. In the dryer, liquid methanol is replaced with liquid $CO_2$. The temperature and pressure are then increased to the super critical point and then vented out of the chamber, thereby leaving a dry, released chip. For drying the chip on the hotplate, the

chip is taken from the HF and rinsed in water before being placed in isopropyl alcohol, which serves to minimize stiction issues during the subsequent baking on a hotplate at 110°C to evaporate the remaining liquid.

## Deployment Mechanisms

Several different deployment mechanisms are available to deploy and retract a MEMS antenna. For this research effort, a MEMS thermal actuator and an electrostatic scratch drive actuator were selected as the basic devices to power the different devices that move the retractable antenna. Both actuation types are discussed in detail in the following sections.

### *Thermal Actuators*

Two methods of locomotion were investigated to power the retracting mechanism: thermal actuators and a scratch drive. A thermal actuator, broadly defined, is a device that produces a lateral or vertical force due to thermal expansion. There are several varieties, ranging from bent-beam thermal actuators, shown in Figure 6, to lateral actuators, shown in Figure 7 [22]. When a current is applied to a bent-beam actuator, the resulting thermal expansion causes the tip to move. Both beams deform to cause the tip to move linearly, whereas a lateral deflection is slightly curved.

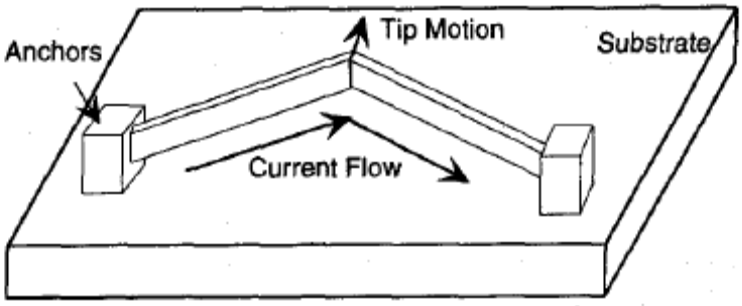


**Figure 6: Bent-beam thermal actuator drawing [22].**

The lateral actuator, which is used in this research, is comprised of two cantilevers made of polysilicon of different widths connected by a bridge at one end. When a current is applied to the device, joule heating causes the structure to move at one end. Due to the smaller cross-sectional area of the hot arm, which is the narrower of the two silicon arms, joule heating results in an expansion larger than the expansion that occurs in the cold arm, thereby causing structural deflection. The unequal expansion in the actuator causes an arc-like movement at the unanchored end. When the current is removed, the actuator returns to its equilibrium position [13].

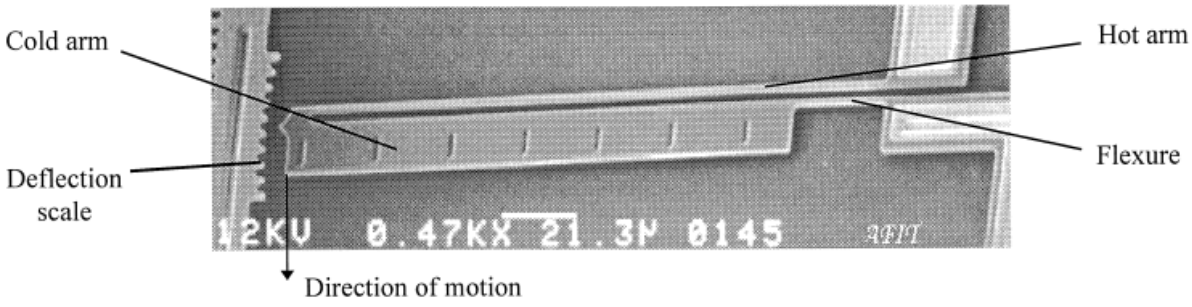


**Figure 7: SEM photo of a lateral thermal actuator [4].**

In lateral actuators, the hot and cold arms are next to each other and are typically made of the same material, so the resulting movement is parallel to the substrate. The width of the hot arm and the flexure are typically 3 μm. In contrast, the hot arms in vertical actuators, shown in Figure 8, are on either side of the cold arms; the resulting movement is in the direction perpendicular to the substrate. The hot arms are Poly1, whereas the cold arm is Poly2 with a Poly0 layer underneath to help ensure the tip deflects upwards. When the current is passed through, the hot arms will expand. Because the PolyMUMPs process is conformal, the expansion of the Poly1 hot arms will force the tip up, since the Poly2 cold arm is in a higher position than the hot arms. Typical vertical actuators can be designed for upwards or downwards deflection, but not both in the same device [29]. The gold is present at the anchored end of the actuator to provide a low resistance contact and help ensure the two hot arms are electrically connected.

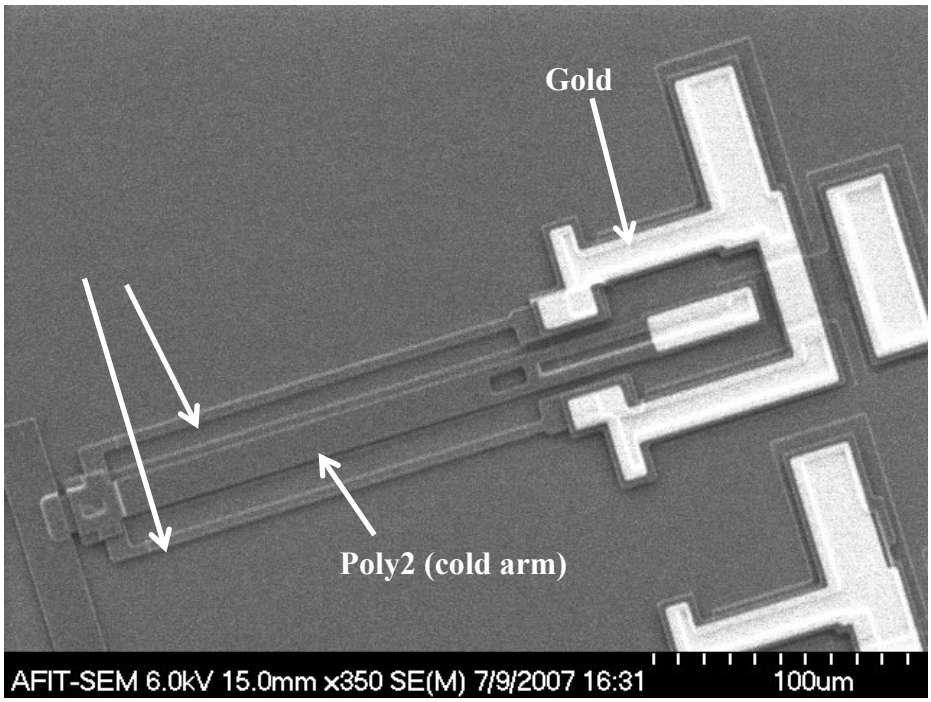


**Figure 8: SEM photo of a vertical thermal actuator.**

It is possible to use an array of thermal actuators to produce a greater amount of force in a microengine. The movable ends of the actuators connect to a yoke that forces the array of actuators to provide a linear directional movement. Figure 9 shows a large bank of Poly1 thermal actuators and its yoke. The other end of the yoke holds a translator, which has teeth to engage the teeth present on the device being moved. Although greater movement can be achieved by increasing the length of a single actuator, such an action increases resistance and decreases force. Additionally, increasing the length of the actuator increases the probability of failure in the actuator due to excessive bowing in the hot arm or the likelihood of stiction, which occurs when a structure adheres to the substrate inadvertently [7].

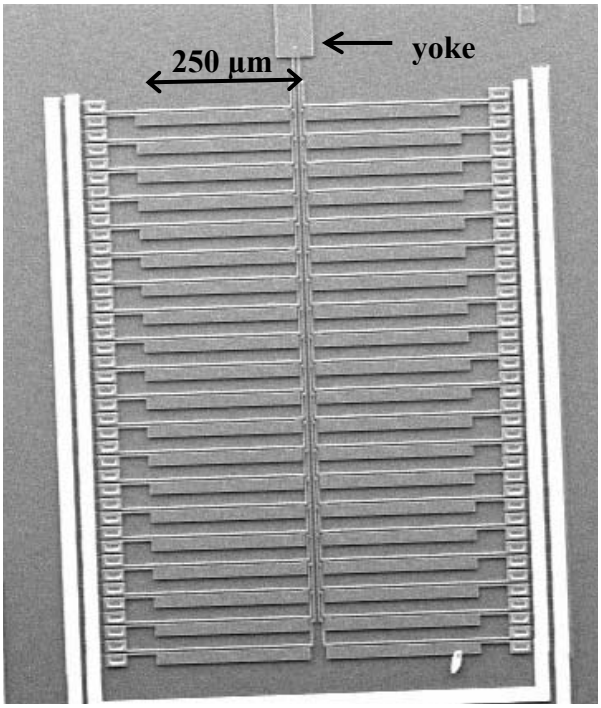


**Figure 9: Array of 40 coupled Poly1 250 µm thermal actuators with yoke.**

In order to supply force in only one direction, one also needs a smaller bank of actuators to operate a pawl that will regulate when the two sets of teeth are engaged. These actuators are also connected to a yoke, but instead of having a translator at the other end, a pawl with a rounded end is used to push on the translator of the larger array [14]. Figure 10 shows how the pawl interacts with the translator when the latter is not engaged. The pawl controls whether the translator engages the teeth on the gear, consequently allowing the thermal actuator array to turn the wheel. Once the thermals have moved as far forward as possible, the pawl pulls back, allowing the translator to return to its equilibrium position of being unengaged. The thermal actuators can then return to their equilibrium position while pulling the translator back without moving the gear. The process then repeats.

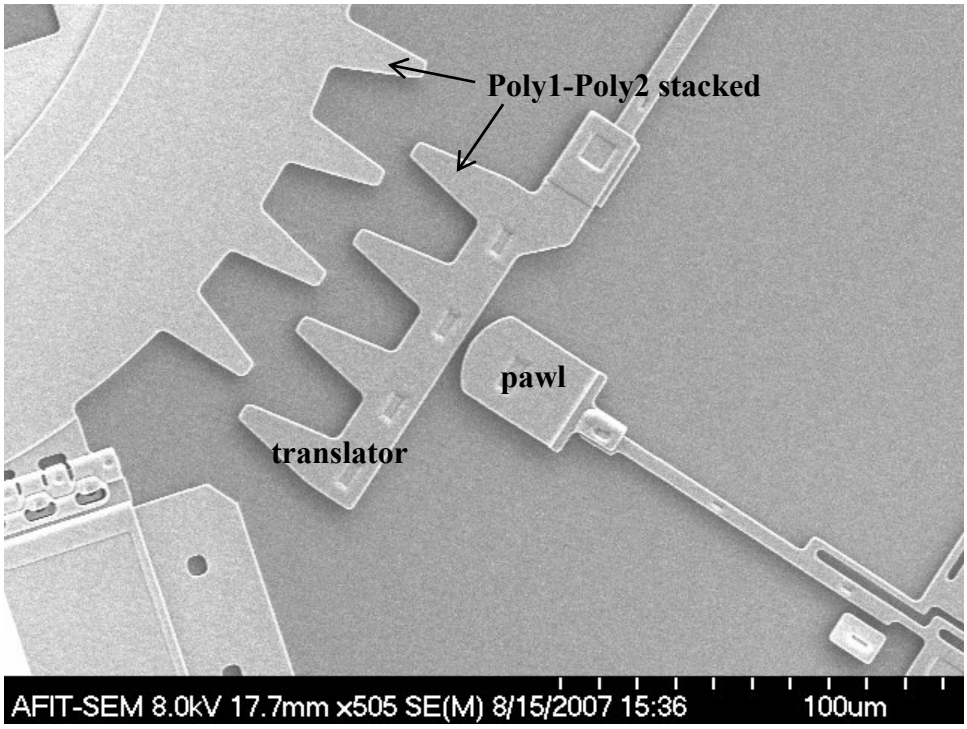


**Figure 10: SEM photo of Poly2 pawl and Poly1-Poly2 translator each with Poly1 yokes interacting with Poly1-Poly2 teeth on a gear.**

It is important to note that when thermal actuators operated to the extent they are overdriven, a phenomenon known as back-bending occurs, which inhibits the device from returning to its original position [28]. The devices become plastically deformed over time, thereby indicating that they should be operated below the overdriven point unless deliberate back-bending is sought, which is the case in this research [7]. Permanent deformation is imminent when the hot arm begins to glow, as shown in Figure 11.

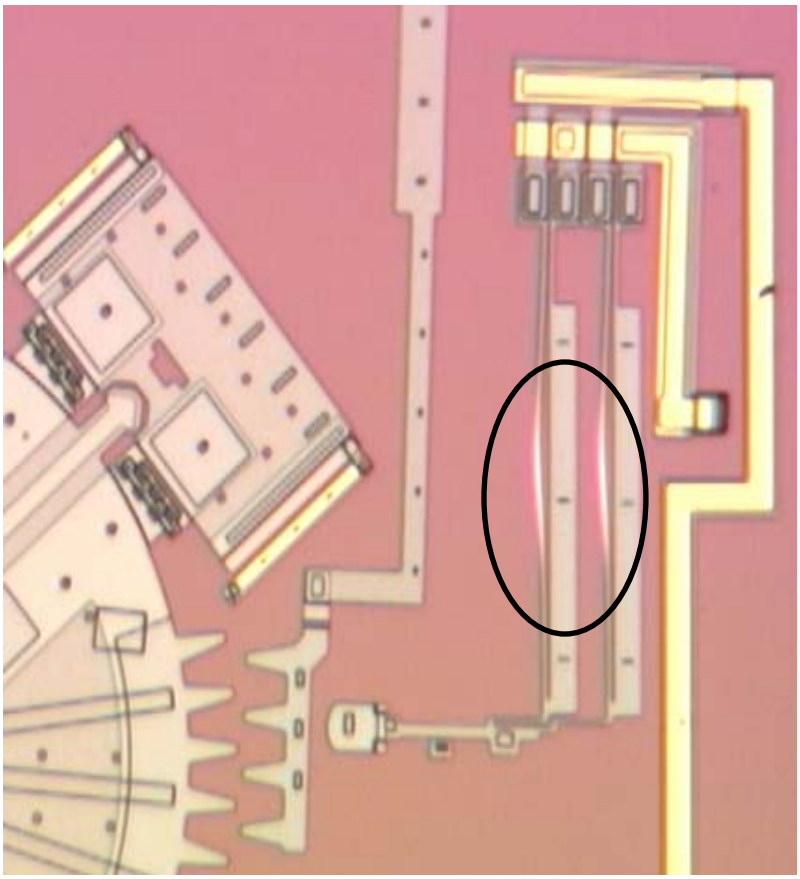

**Figure 11: Poly1 lateral thermal actuators illustrating joule heating of the hot arm, creating lateral deformation.**

Thermal actuators are useful in that they can yield a high force with a relatively low voltage. However, they are not very suitable for motion faster than 75 Hz due to the extreme amount of back-bending that occurs near and beyond that frequency. A complete thermal actuator microengine is shown in Figure 12. One set of actuators controls the pawl, while the other set controls the translator.

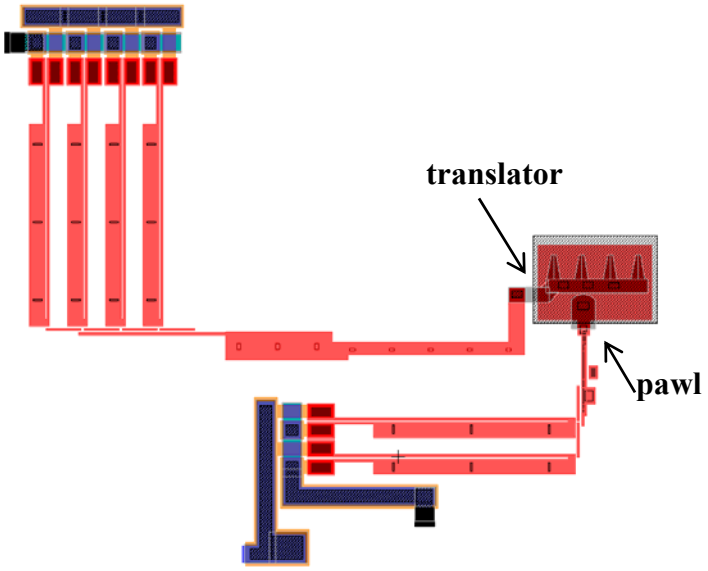


**Figure 12: L-Edit schematic of 250 µm Poly1 lateral thermal actuator microengine.**

***Scratch Drives***

Electrostatic forces between a plate and the substrate compel a scratch drive to move when a voltage is applied. The scratch drive plate has a perpendicular foot called a bushing that rests on the substrate to form a triangle. The electrostatic force increases as charge accumulates between the plate and the ground electrode, often the substrate, until it deforms and snaps down to the substrate, forcing the bushing to move outward. When the charge dissipates, the foot remains in contact with the substrate, while the plate returns to its original position, although it has moved forward. This motion, diagrammed in Figure 13, is similar to that of an inchworm, with the foot resembling the front part of the worm and the plate resembling the rear part. Scratch drives have been used in RF microswitches as contacts and in variable capacitors as motors [6].

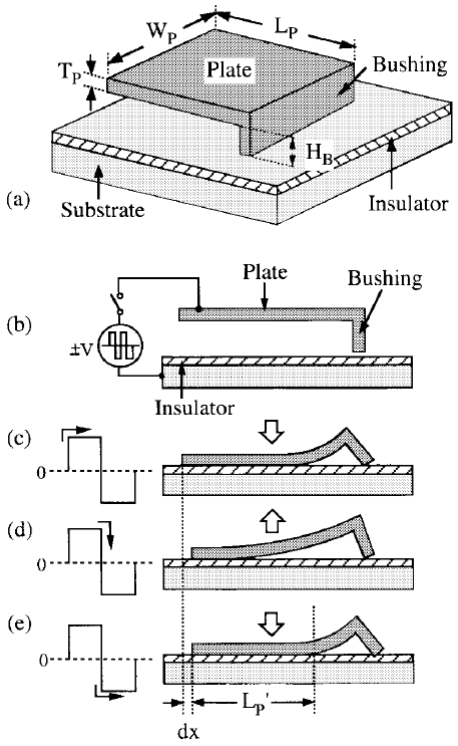


**Figure 13: Scratch Drive Actuator Operation [1].**

One benefit of the scratch drive is that it can be operated at a high frequency, which in turn means it moves at a faster pace than a thermal actuator. However, scratch drives also have a low power requirement.

### Three Dimensional Structures

True three-dimensional structures can be very difficult to create in the standard MEMS fabrication processes. Oftentimes, a micromanipulator is used to assemble hinged structures to create such a 3-D device. Such construction methods are not always fruitful, as structures can easily be damaged or are not conducive to being moved by probe tips. Furthermore, such tedious processes are not suitable for large-scale

production. It is possible to add other MEMS devices that facilitate self-assembly or to obtain the desired 3-D structure [10]. In fact, a scratch drive-powered device has been fabricated that lifted structures approximately 150 μm [1]. However, sometimes these supplemental structures for 3-D assembly are too large or complex to be successfully implemented, meaning that hand-assembly is necessary to create the 3-D structure.

Microhinges have been used to create a variety of flip-up structures. One group of scientists utilized them, along with a vertical thermal actuator, linear assembly micromotor, and a locking mechanism, to create a scanning micromirror and cube reflector system. The thermal actuator lifts the mirror plate a small amount, putting it in a position for the linear motor to finish the job. Once the plate has been raised to its position, the locking mechanism slips into a hole on the plate and prevents the plate from returning to its original position [23]. One such locking mechanism used in conjunction with a hinge is shown in Figure 14. The Poly1 portion of the hinge is held in place by the Poly2 covering. The Poly2 lock fits through the gap in Poly1 and locks into place, preventing the raised portion of the hinge from returning to its original position without first being raised.

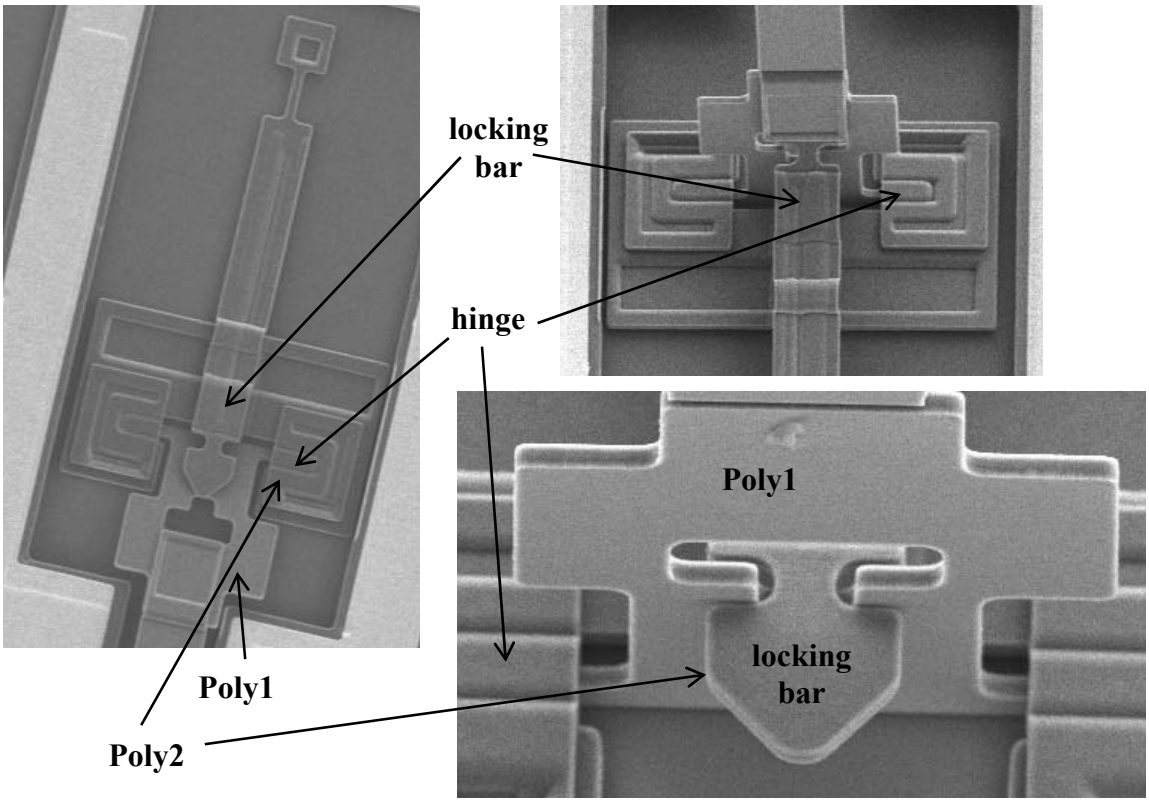


**Figure 14: Hinge and Poly2 locking mechanism before (left) and after (right) assembly. The top right figure shows the back view of the lock and hinges, while the bottom right figure shows the front view.**

In addition to hinges comprised of two pieces at a particular angle to each other, elastic hinges have also been used, where the Lorentz force directs how the hinge bends, as diagrammed in Figure 15 [24]. A 3-D structure can be created by applying an appropriate magnetic field to fold the appropriate hinges.

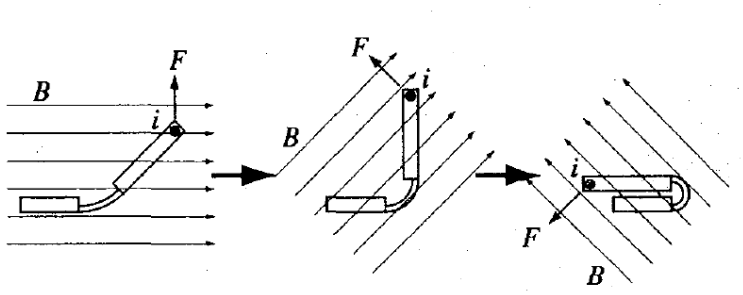


**Figure 15: Diagram of elastic hinges controlled by Lorentz Force [24].**

A method using cured polyimides to assemble 3-D structures has also been developed. This process easily allows for electrical connections and choosing the desired angle of the raised structure. In short, the material is put in a V-shaped groove and cured, shrinking the material, thereby drawing the two sides of the V closer together [9]. Conducting polymers have also been used as hinge materials, allowing an electrical current in a reversible process to control how much bend exists in the material. However, the hinge must be at all times in contact with an electrolyte, which means that it would need to be submerged in an aqueous salt solution, for example [25].

Similar to the polyimide method, another way to create three-dimensional systems involves using molten solder, glass, or photoresist [5, 11, 26, 27]. A hinged plate with a metal pad has a solder ball placed between it and a metal pad on the substrate, at which point the temperature is raised to the solder's melting point. The left-hand picture in Figure 16 shows a 3-D structure utilizing solder balls. The surface tension forces the plate to move to its desired location, which is determined by the amount of solder used and the position of the metallized pads. Sometimes, a kickstand lock is also present to aid in specifying the desired angle, as shown in the right-hand diagram in Figure 16.

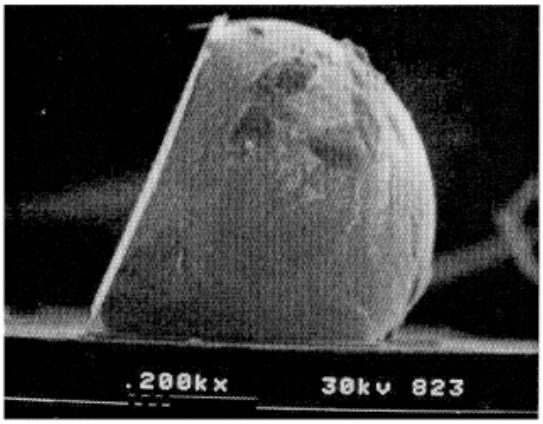


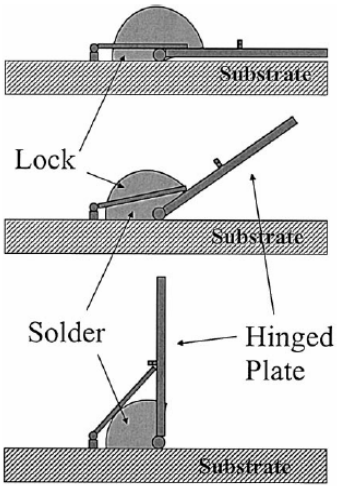


**Figure 16: SEM photo (right) and diagram (left) of a solder ball being used in conjunction with a hinge [11]. The locking mechanism is typically to the side of the solder ball if they are used in conjunction.**

**Summary**

Developing an antenna for use on microrobots or insects is of interest due to the necessities of communication with the MEMS device or system. To further these ends, research into the design of an antenna that could fulfill such a purpose has been conducted. Several concepts highlight themselves in importance to these goals, including scratch drives and thermal actuators for the engine and solder balls, hinges, and locks for the antenna assembly.

# III. Methodology

## Chapter Overview

In this chapter, the process used to develop the different designs for the mechanisms for antenna deployment are detailed. The type of antenna for which the mechanisms are to be designed is also explained. Finally, descriptions of the different designs themselves are included.

## Antenna

In order to design a microsystem to deploy and retract an antenna, an idea must exist of the type of antenna for which to design the system, since the sponsor supplied no particulars about the antenna. There are a myriad of antenna types that exist, including Yagi, panel, loop, and dipole antennas. The size, complexity, and directivity of the desired antenna must also be considered. A directional antenna would either disallow communication at certain times when the antenna was not oriented correctly, or require extra circuitry to move the antenna to a position that would enable communication. An antenna requiring a complex design would likely also require extensive circuitry and space to facilitate its movement. Because of the problems associated with complex and directional antennas, a simple monopole was selected as the type of antenna around which this system would be designed.

The next decision to make was the desired length of the antenna. Looking at Table 1, it can be seen that in order to remain within the radio frequencies and not delve into the infrared, while at the same time keeping the antenna small enough that it can be

easily manipulated by a MEMS device, an antenna for a frequency greater than 50 GHz must be designed.

**Table 1: Antenna lengths for various frequencies and dipoles**

| | Full-wave | Half-wave | Quarter-wave |
|---|---|---|---|
| Frequency (GHz) | Length (mm) | Length (mm) | Length (mm) |
| 1 | 300 | 150 | 75 |
| 5 | 60 | 30 | 15 |
| 10 | 30 | 15 | 7.5 |
| 50 | 6 | 3 | 1.5 |
| 100 | 3 | 1.5 | 0.75 |
| 300 | 1 | 0.5 | 0.25 |

Due to the small nature of an insect and the limitations of the PolyMUMPs process, the length of the antenna cannot be large. For the purposes of this proof-of-concept design, a length of 1 mm was chosen. The wavelength of a signal is given by:

$$\lambda = \frac{c}{f} \tag{3.1}$$

where $c$ is the speed of light, $3x10^8$ m/s, $\lambda$ is the wavelength in m, and $f$ is the frequency in Hz. The type of dipole – full, half, or quarter-wave – determines the factor by which the wavelength may be divided to obtain the length of an antenna able to receive that signal. In this instance, a 1 mm antenna can be used to receive a 300, 150, or 75 GHz signal.

**Designs**

The MEMS redeployable antenna mechanisms designed, fabricated, and tested throughout this research effort are described in the following sections. The functionality of each device is also explained.

### *Array of Gears and Beams*

Once an approximate antenna length was chosen, work on the actual designs could begin. The first idea conceived was that of an array of gears and beams. Shown in Figure 17, the design is comprised of five beams separated by four gears.

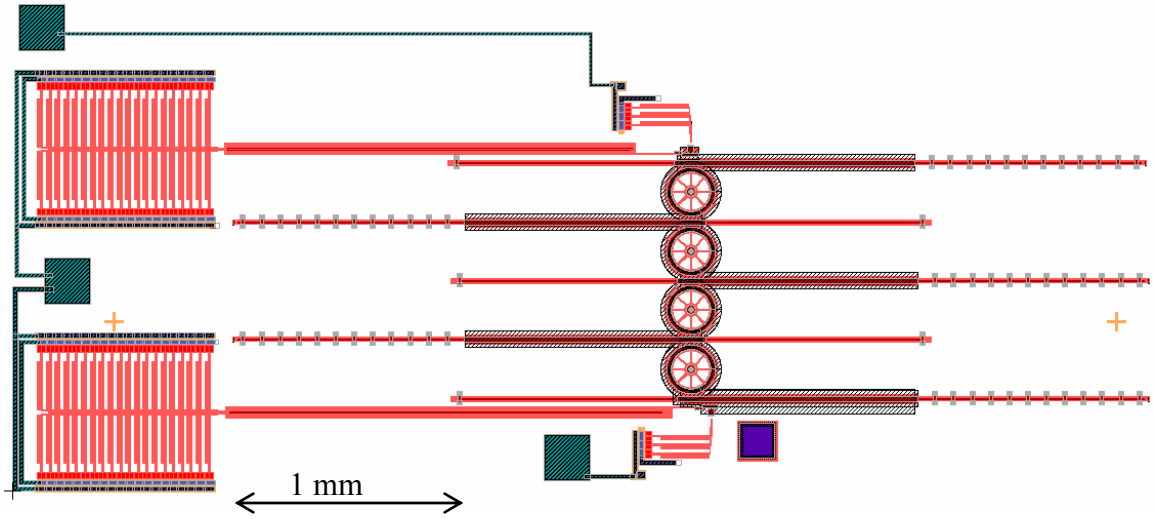


**Figure 17: L-Edit design of gears and beams with thermal actuator microengine.**

The gears serve two main purposes: they separate the beams, thereby reducing the amount the antenna must be curved, and force the beams to move in opposite directions. The antenna, a gold wire, will be attached to the substrate at the metal bonding pad, represented by the purple square in Figure 17. It should snake through two metal posts that are located on one end of each of the beams. The beams that interact with the gears have two features: they provide a location for guideposts, shown in Figure 18, that keep the antenna in place and have a Poly1 extension that keeps the beam from

translating too far or moving in an undesired direction. The posts will need some more metal deposited in a post-processing step in order to achieve a height great enough to serve as guides for the antenna.

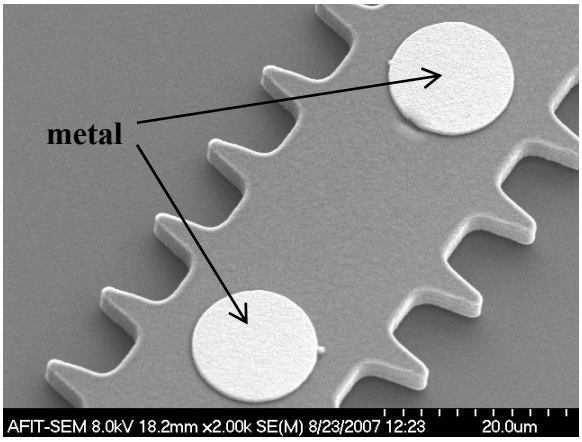


**Figure 18: Metal posts on Poly1-Poly2 stacked beam.**

These post positions are alternated on each side of the gear, allowing the undeployed antenna to make a shape like that in Figure 19.

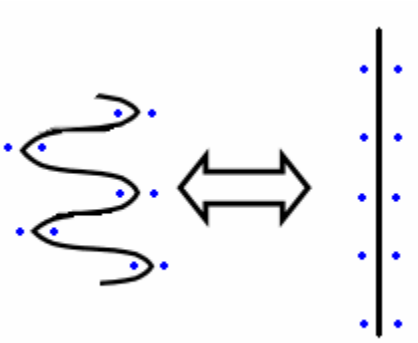

**Figure 19: Concept drawing of antenna shape in retracted (left) and deployed (right) position using the gears and beams deployment scheme. The blue dots represent the posts to hold the antenna in place.**

The beams are moved into the desired position via two thermal actuator engines. One engine controls the movement of the top-most beam, while the other controls the bottom-most beam. The movement of the end beams needs to be coordinated, as each forces the adjoining gear to move, which in turn engages the teeth on the beam located on the opposite side of the wheel. Moving from the undeployed to the deployed position means that the bottom wheel would be turned in the clockwise direction, while the top wheel would have to move in the counterclockwise direction. Movement ceases when the posts are in a position such that a straight line could be drawn through each set of posts and each gear. The wire would then be extruded in a straight manner. Due to the fragile nature of these devices and the fact that they had a tendency to break during the releasing process, these devices were never tested.

***Hinged Wheel***

The next design is similar to a hose reel. A gear has four hinged flaps arrayed around it so that they can be lifted perpendicular to the gear. The device, once fully assembled, should resemble Figure 20. The antenna is bonded to a metal pad located on the wheel. It is then wrapped around the outside of the flaps similar to the way a hose is wound around its reel.

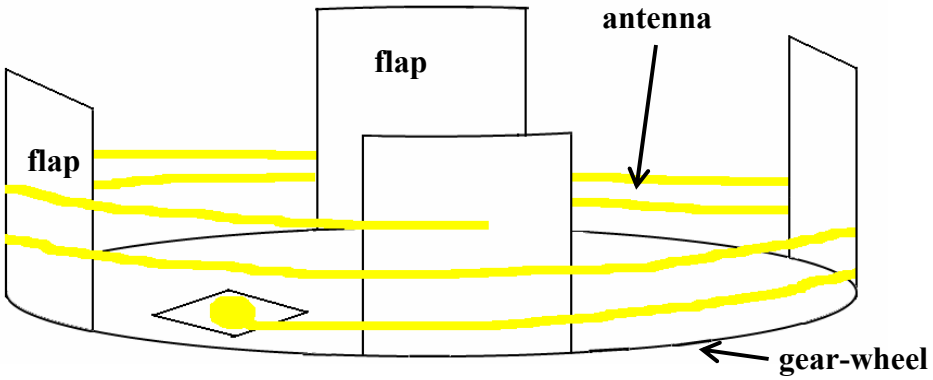


**Figure 20: Concept drawing of hinged wheel with antenna.**

In one version of the design, shown in Figure 21, a locking mechanism holds each flap in position once it is manually raised by a microprobe tip. The prominent squares on the flap serve to connect the Poly1 flap to the Poly2 portion of the hinge.

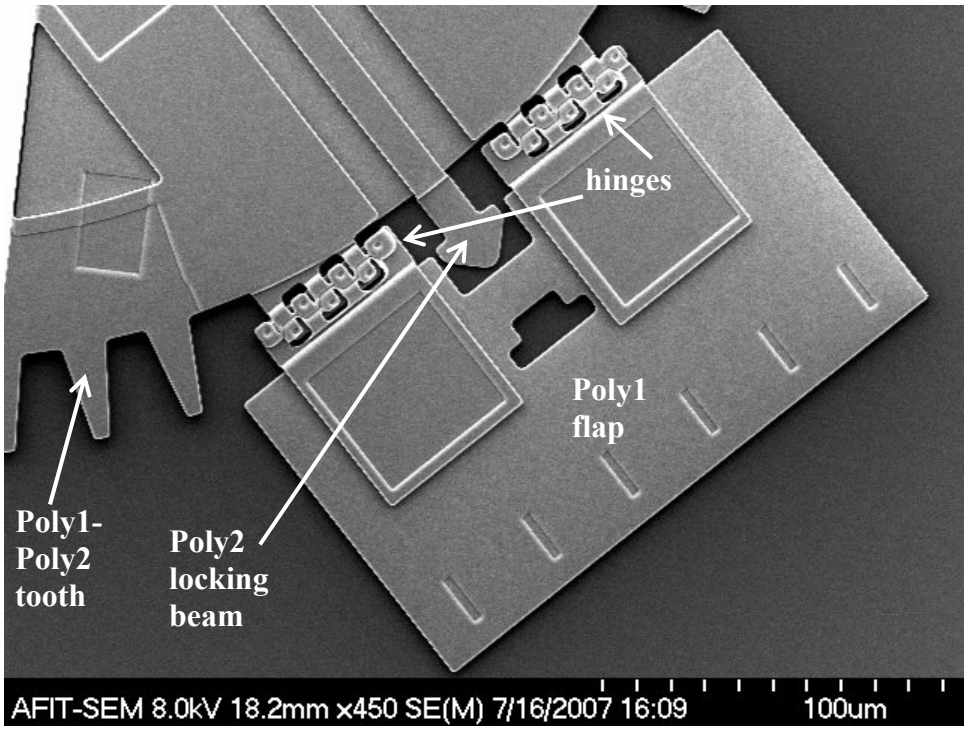


**Figure 21: SEM photo of flap of hinged wheel with locking mechanism.**

Another version of this design has the flaps being raised and held in place using the surface tension of solidifying solder. Figure 22 shows a flap from one such system. The two prominent lighter squares are the metal pads where the solder ball will be attached to raise the flap.

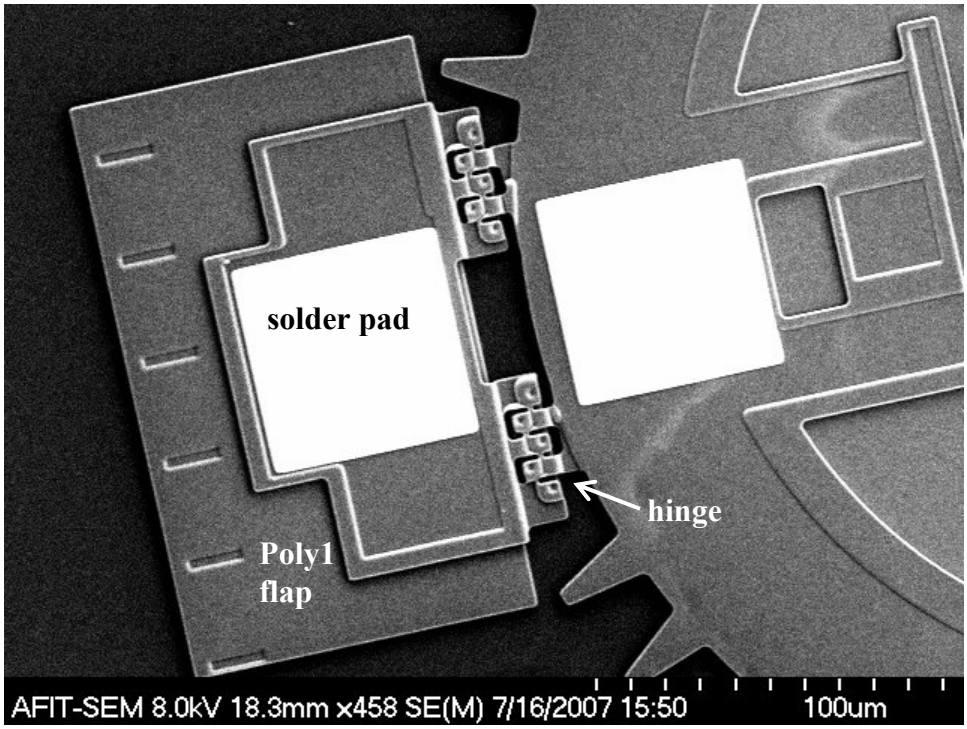


**Figure 22: SEM photo of hinged wheel flap with solder pads.**

An additional version of the hinged wheel is shown in Figure 23 and includes residual stress cantilevers on the sides of the flaps to aid in assembly of the 3-D structure. The cantilevers serve to elevate one end of the flap in order to make it easier to slip a probe tip underneath to lift the flap into position.

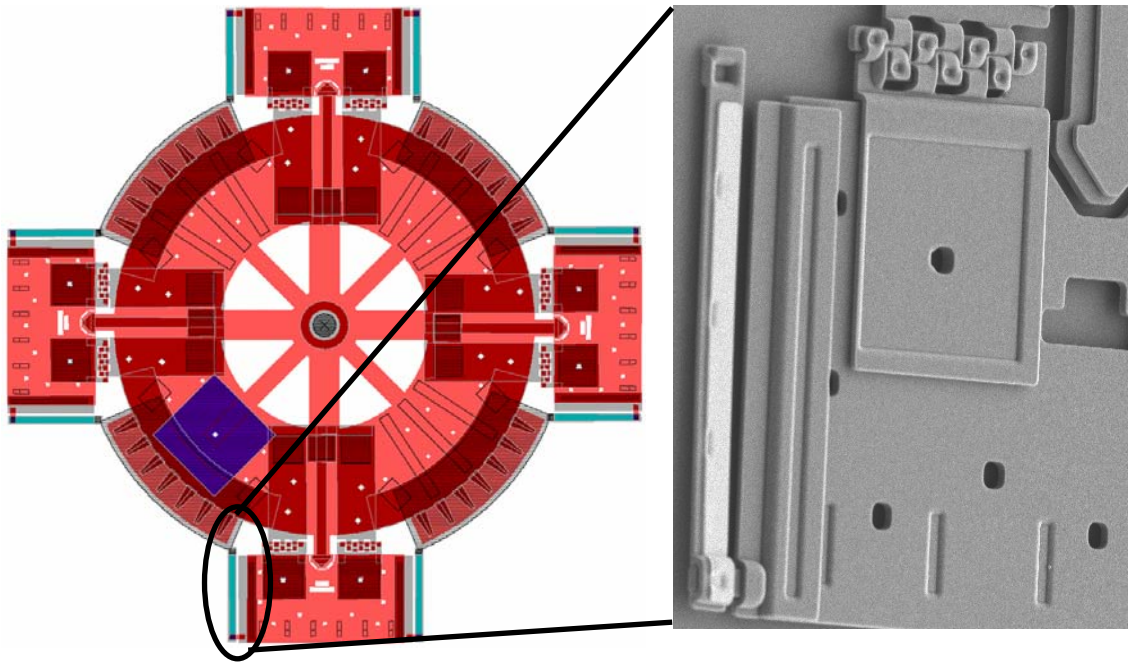

**Figure 23: L-Edit design (left) of hinged wheel with SEM photo of 100 µm residual stress cantilever that aids in self-assembly.**

Two banks of thermal actuators power the movement of the wheel in both the clockwise and counterclockwise directions. The version of the wheel with locking flaps and its powering mechanism is shown in Figure 24.

However, the nature of the wire was not taken into account with these designs that require the antenna to be wound. Because the wire is so small, with a diameter of 10 µm, it is extremely malleable. For this reason, when the wire bends, it will most likely stay bent until something deliberately unbends it. Therefore, the array of gears and beams design and the hinged wheel design have the inherent flaw that once the antenna is in a retracted position, it could become very difficult to straighten out and use as a monopole antenna. Modifying the antenna so that it has a little more rigidity, such as by adding some supporting Poly2 in regular intervals, could help mitigate this problem.

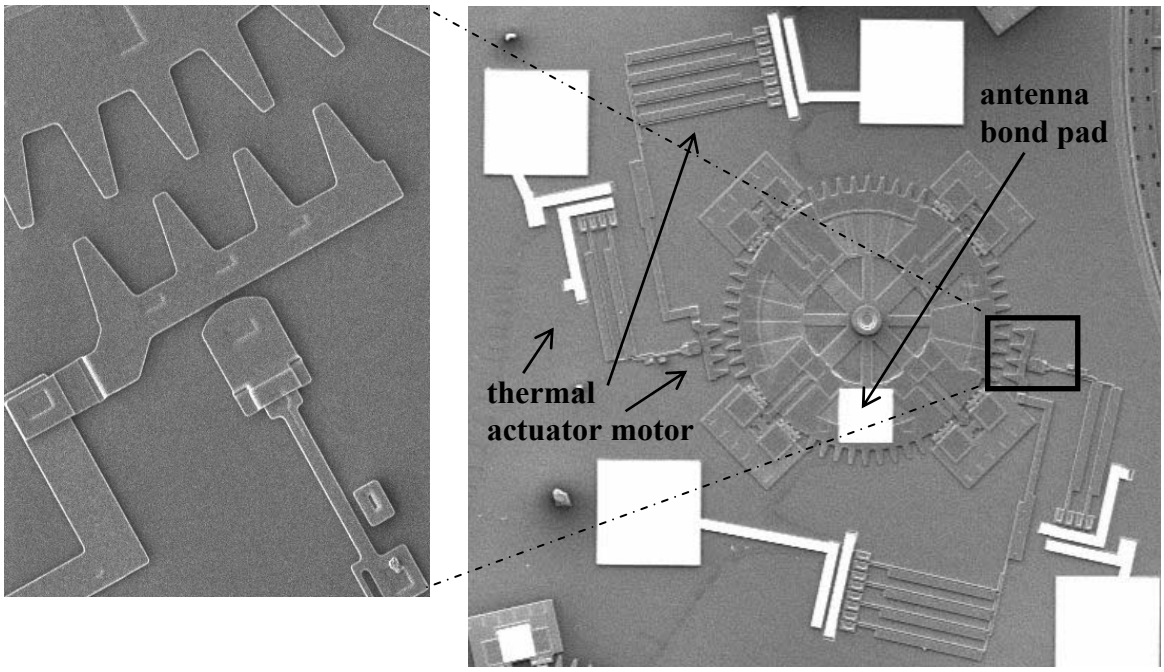


**Figure 24: SEM photo of unassembled hinged wheel with thermal actuator motor.**

***Large Wheel***

Because of this flaw of the bent wire, a larger wheel design was created, shown in Figure 25. Instead of having a diameter of approximately 500 μm like the smaller hinged wheels, the large wheel has a diameter of approximately 3 mm. However, the large wheel was only designed to have the wire wrapped around it one time. Instead of having flaps that are raised up for the wire to wrap around, it has a trench through which the wire is to be threaded. The trench has guide posts at a regular interval along it that help keep the antenna in the trench. A post-processing step could add a layer to the top of these posts, creating a bridge to keep the antenna in the trench. This wheel is powered by two rings of scratch drives inside the wheel. The major drawbacks to this design are that it is

so large and that the scratch drives are arrayed such that they can only turn in one direction, meaning the antenna cannot be retracted.

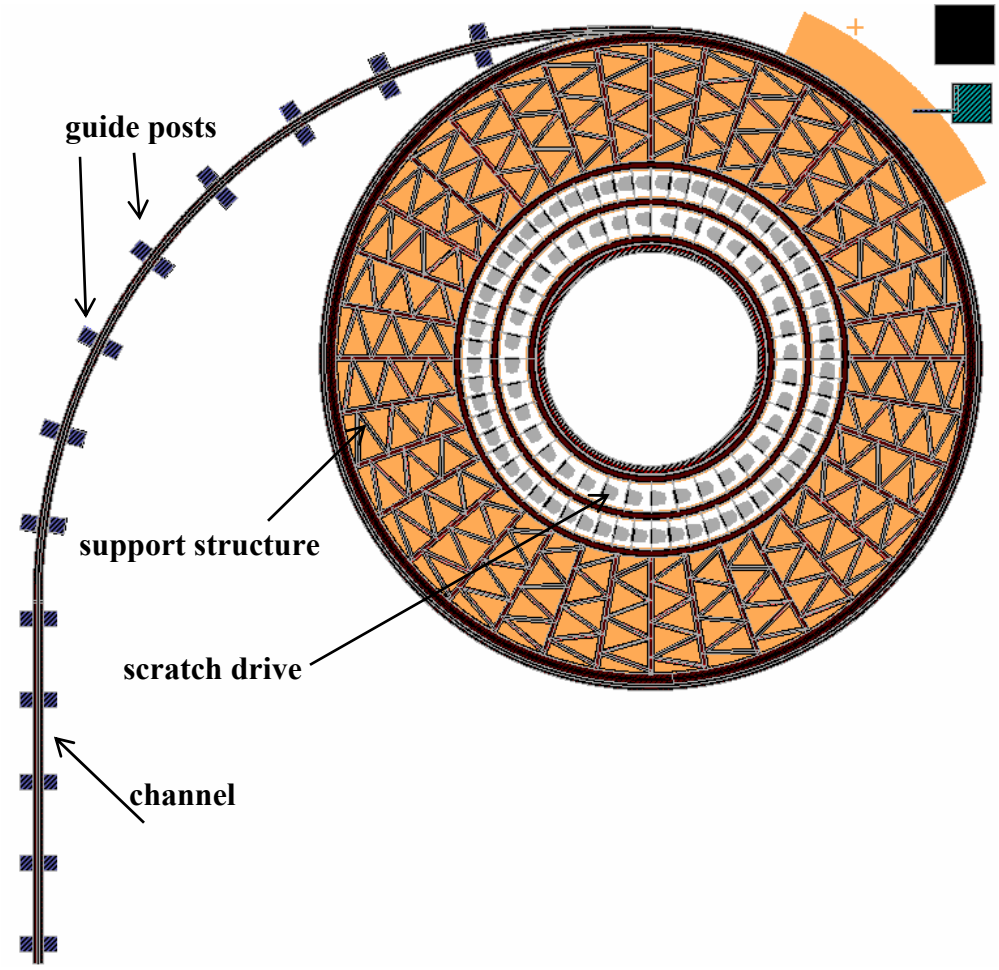


**Figure 25: L-Edit drawing of large 3 mm wheel design with scratch drive motor actuation.**

Using the best parts of the hinged wheel and the large wheel, another basic design was developed. Both variations of this hybrid design were not practical and are detailed in Appendix B.

***Vertical Beam***

The next design envisioned was a simple 1 mm long beam that was raised to a position approximately perpendicular to the substrate. One version of this design has vertical thermal actuators that one by one raise the beam a fraction, starting from the tip. A lock holds the beam in place and a spring is connected to the end to pull the beam back to the substrate when the designated vertical thermal actuator disengages the lock. The lock, spring, and two of the powering vertical thermal actuators are shown in Figure 26.

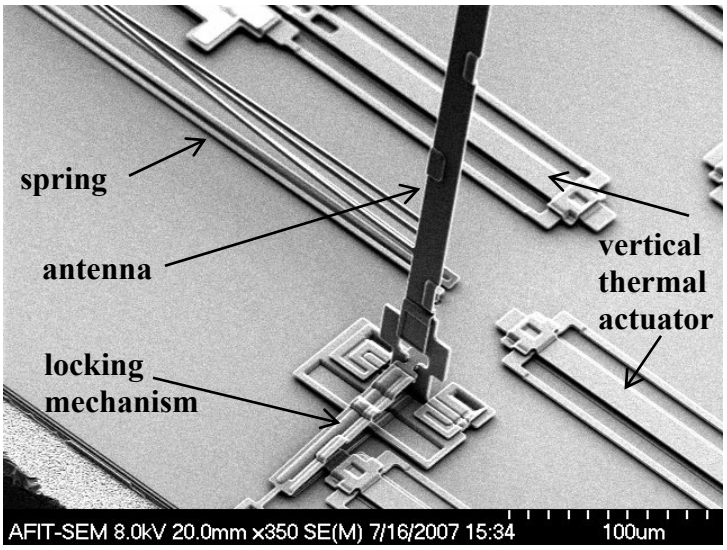


**Figure 26: SEM photo of beam antenna with lock and spring.**

Another variation of the 1 mm beam design, shown in Figure 27, has the beam being raised into position via residual stress cantilevers, made of Poly2 and gold. Three different variations were fabricated: the cantilevers are either 40, 60, or 80 μm wide.

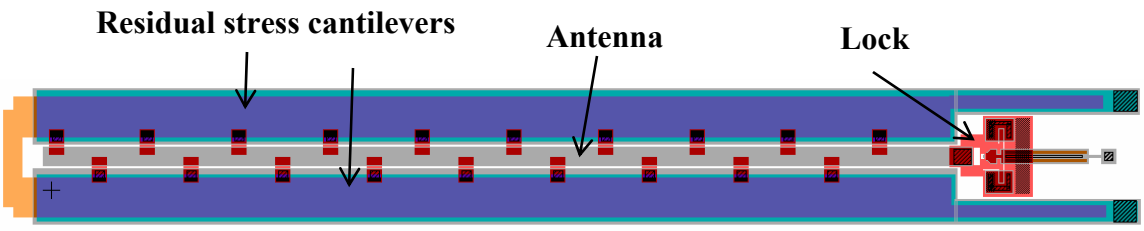


**Figure 27: L-Edit layout of residual stress 1 mm beam antenna.**

It is important to note that the raised indentations on the antenna from the tabs on the vertical actuators or residual stress cantilevers could cause some changes to the antenna pattern. Although the gain from this design would principally be concentrated on the front and back sides of the antenna, which are 10 μm across, instead of the thin edges, which are only 1.5 μm across, the indentations, were they still present when the metal for the actual antenna was deposited, could cause more radiation in those side directions and less radiation from the front and rear sides.

***Translated Beam***

The final design again involved a 1mm long beam. This beam, instead of being moved vertical to the substrate, is translated so the end of the antenna comes off the chip and can then be retracted. One gear on each side of the beam is turned by a bank of thermal actuators, while all the gears serve to keep the beam moving only in the horizontal direction, as shown in Figure 28.

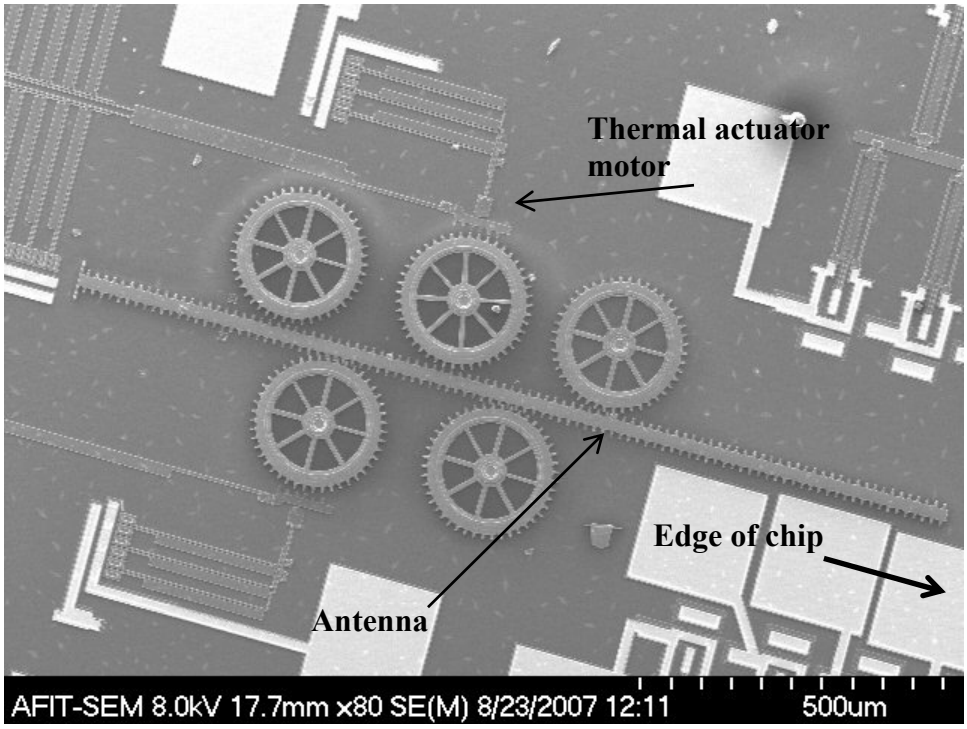


**Figure 28: SEM photo of horizontally translated 1mm Poly2 beam with chip edge direction indicated.**

In order to improve this device and enable it to be tested, the gears and their corresponding motors need to be moved slightly, on the order of a few microns, inward toward the beam so that the beam cannot shift and is forced to move when the gears turn. Also, adding staples or railings to the edge of the beam to help keep it from disappearing off the chip during the releasing process would be beneficial.

**Summary**

This chapter refines the set task of developing a retractable microantenna and details the different designs created. The array of gears and beams, large wheel, hinged wheel with flaps, 1mm vertical antenna, and 1mm horizontal antenna are the main designs explained.

# IV. Analysis and Results

## Chapter Overview

This chapter discusses the results obtained in testing each device. Thermal actuators, residual stress cantilevers, and hinges are among the components to be addressed in more detail in this section.

## Theory

In order to determine how much deflection can be expected out of a polysilicon cantilever with a thin film on top, one begins with Stoney's equation

$$\sigma_{res} = \frac{E_p' t_p^2}{6 t_f R} \Rightarrow \frac{\sigma_{res} 6 t_f}{E_p' t_p^2} = \frac{1}{R}. \tag{4.1}$$

This equation takes into account parameters of a cantilever, including the radius of curvature $R$; the thickness of the polysilicon and film layers $t_p$ and $t_f$; and the biaxial modulus of polysilicon $E'_p$. It is important to note that this equation was developed to model stresses across an entire wafer, not localized stresses in a cantilever. Nevertheless, its guiding principles remain the same. The residual stress $\sigma_{res}$, which is a wafer-wide value given by the manufacturer for a particular run number, is also equal to the sum of the internal fabrication stress $\sigma_{int}$ and thermal stresses due to the misfit strain between the two layers $\sigma_{th}$. The thermal stresses can be represented by

$$\sigma_{th} = E_f' \left(\alpha_p - \alpha_f\right)\left(T - T_o\right) \tag{4.2}$$

where $E'_f$ is the biaxial modulus of the thin film; $\alpha_p$ and $\alpha_f$ are the thermal expansion coefficients for polysilicon and the film, respectively; $T$ is the temperature at which the

beams are being investigated; and $T_o$ is the temperature at which the thin film was deposited when the misfit strain was zero. The radius of curvature $R$ is also defined by

$$\frac{1}{R} = \frac{M}{EI} = \frac{d^2 y}{dx^2} \tag{4.3}$$

where $M$ is the moment acting on the cantilever; $I$ is the moment of inertia; and $x$ and $y$ represent the directions along the length and the height of the beam, respectively. Integrating (4.3) yields

$$y = \frac{Mx^2}{2EI} = \frac{x^2}{2R} \tag{4.4}$$

into which the left-hand side of (4.3) is substituted to find $R$ in terms of $x$ and $y$. This expression for $R$ is then substituted into (4.1) to yield

$$y = \frac{3t_f \sigma_{res} x^2}{E_p^{'} t_p^2} \tag{4.5}$$

which describes the vertical displacement of a cantilever as a function of length.

To determine how much lateral deflection $\delta_{lateral}$ one can expect out of the tip of a lateral thermal actuator, one can use this equation:

$$\delta_{lateral} = \frac{3L^2 (T_{hot} - T_{cold})[\lambda(T_{hot}) - \lambda(T_{cold})]}{4w_{h+f}} \tag{4.6}$$

in which $L$ is the length of the hot arm; $T_{hot}$ is the average temperature of the hot arm; $T_{cold}$ is the average temperature of the cold arm; $\lambda(T_{hot})$ is the coefficient of thermal expansion (CTE) for polysilicon at the average hot arm temperature; $\lambda(T_{cold})$ is the

coefficient of thermal expansion for polysilicon at the average cold arm temperature; and $w_{h+f}$ is the sum of the widths of the hot arm and the flexure holding the cold arm.

**Calculations and Measurements**

The following sections discuss the deflection of residual stress cantilevers and both lateral and vertical thermal actuators. Additionally, a discussion about the potential speed of deployment of the hinged wheel is included.

***Residual Stress Cantilevers***

Residual stress cantilevers can aid in lifting up structures. In order to estimate how much a structure can be raised by such cantilevers, the deflection of such a structure can be calculated using equation (4.5). Five cantilevers made of different PolyMUMPs layers ranging in size from 50 to 250 μm were investigated. It was found that the Poly2-gold cantilevers had more upward deflection than the Poly1-Poly2-gold, Poly1, or Poly2 cantilevers. The latter two types of cantilevers have stress gradients resulting from the doping of the polysilicon layers during the fabrication process that cause the bending. The Poly1-Poly2-gold cantilevers had a greater thickness of polysilicon, thereby making it more difficult for the residual stress to bend the cantilevers, resulting in a smaller deflection. Hand calculated deflections, as well as the actual measured deflections for the Poly2-gold cantilevers, are shown in Table 2.

**Table 2: Poly2-gold cantilever deflections.**

| | Deflection(μm) | | |
|---|---|---|---|
| **Beam length (μm)** | **Calculated** | **Measured** | **% error** |
| 50 | 0.37011 | 0.4389715 | 18.6056848 |
| 100 | 1.48046 | 1.23919 | 16.29696176 |
| 150 | 3.33104 | 2.9023325 | 12.87007961 |
| 200 | 5.92185 | 4.7608 | 19.60620414 |
| 250 | 9.2529 | 7.0352925 | 23.96662128 |

The best-fit curve for the measured deflection values is

$$y = 0.00008984x^2 + 0.006482x - 0.167 \tag{4.7}$$

and is plotted in Figure 29. This plot shows a deflection of approximately 96 μm for a millimeter-long Poly2-gold beam. This plot also indicates that a 1.2 mm Poly2-gold cantilever would have an upward deflection of approximately 137 μm.

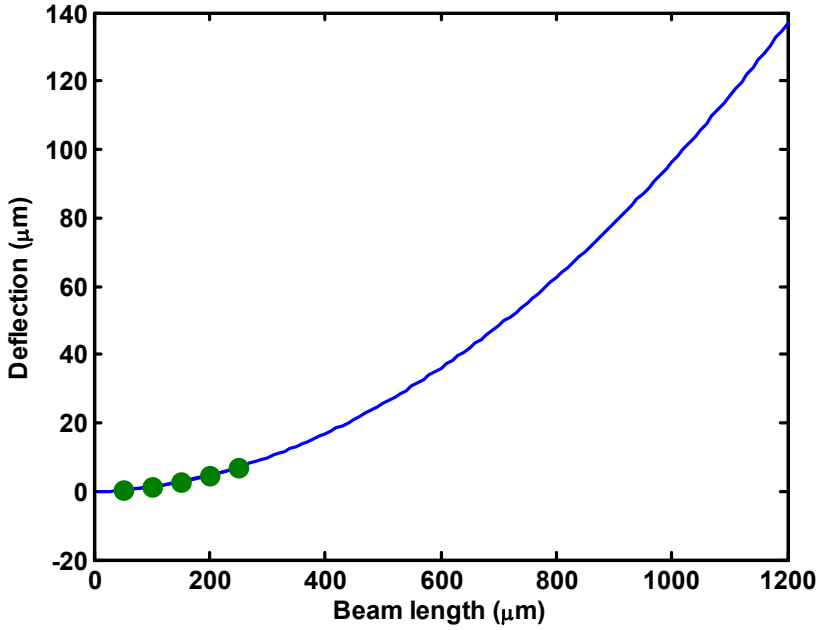


**Figure 29: Predicted deflection for Poly2-gold cantilevers based on measured data.**

### *Lateral Thermal Actuators*

Lateral thermal actuators are a key component in the microengines used in several of the aforementioned designs. In order to determine the best length for the actuators comprising the arrays, tests on individual Poly1 lateral thermal actuators of various lengths were performed. The maximum tip deflection of the lateral thermal actuators and the predicted deflection values are shown in Table 3. The calculated values were figured estimating the hot arm temperature at 1000 K and the cold arm temperature at 300 K, giving a CTE of 4.31e-6 $K^{-1}$ and 2.616e-6 $K^{-1}$ for the hot and cold arms respectively [12].

**Table 3: Poly1 lateral actuator maximum deflections.**

| | **Deflections (μm)** | | |
|---|---|---|---|
| **Length (μm)** | **Calculated** | **Measured** | **% error** |
| 120 | 2.561328 | 6 | 134.2542 |
| 147 | 3.843593 | 8 | 108.1386 |
| 184 | 6.021967 | 10 | 66.0587 |
| 211 | 7.918950 | 13 | 64.16318 |
| 230 | 9.409323 | 14 | 48.7886 |
| 257 | 11.74814 | 16 | 36.19177 |
| 293 | 15.26996 | 20 | 30.97611 |
| 321 | 18.32790 | 23 | 25.49174 |

Differences between the calculated and measured deflections are likely due to differences in the assumed and actual average temperatures of the hot and cold arms and the corresponding CTEs. The average measured tip deflection in Poly1 lateral thermal actuators of different lengths for different voltages is shown in Figure 30.

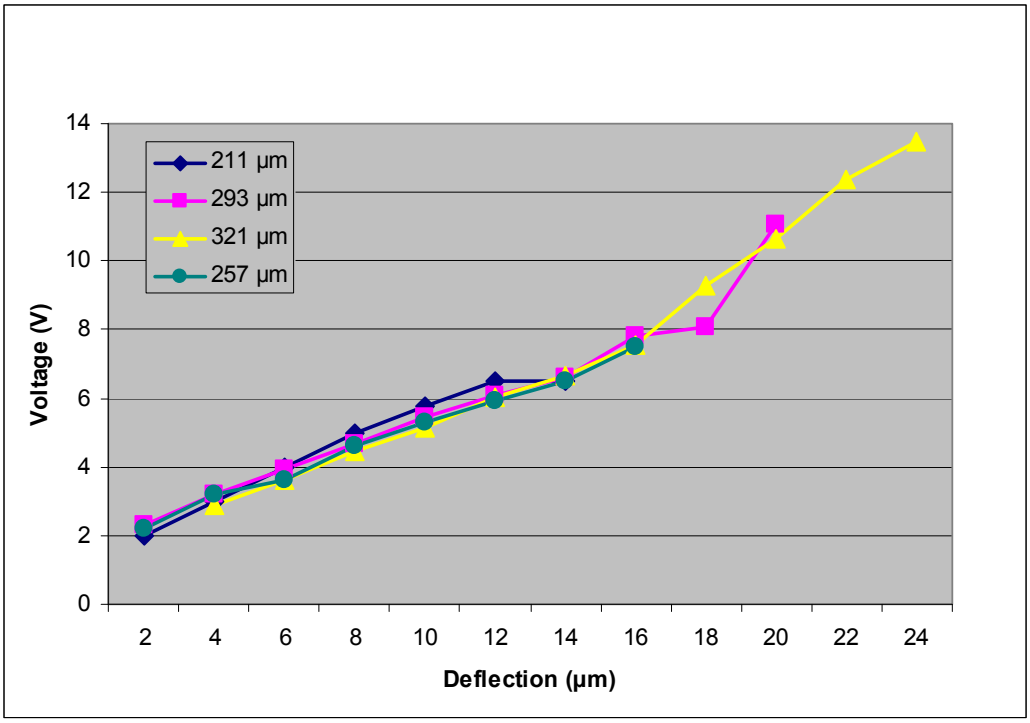


**Figure 30: Poly1 lateral thermal actuator tip displacement for varying actuator lengths.**

The 321 µm actuators had the largest displacement but had some stiction issues, despite the presence of dimples, that resulted in noticeably jerky movements. Although not as severe as in the 321 µm actuators, the 293 µm actuators also moved as if they sometimes were temporarily adhered to the substrate, despite the presence of dimples. The 211 µm actuators, on the other hand, moved smoothly and consistently. The 257 µm actuators paralleled the amount of deflection for a given voltage that the two longer actuators had, though they had a lower burnout voltage. However, these actuators did not have stiction issues. Given that the thermal actuators, when joined together, will have the extra weight of the yoke on their unanchored end, it is not prudent to use an actuator that has stiction problems when tested individually. An actuator with a length of 250 µm was

chosen as the backbone of the thermal actuator engine arrays because it is shorter than the ones with stiction problems yet long enough to yield a significant deflection.

***Vertical Thermal Actuators***

Under the Zygo, deflections of the vertical actuator tip were measured as a bias was applied. From the results of this testing, depicted in Figure 31, it was realized that the actuators did not work as designed.

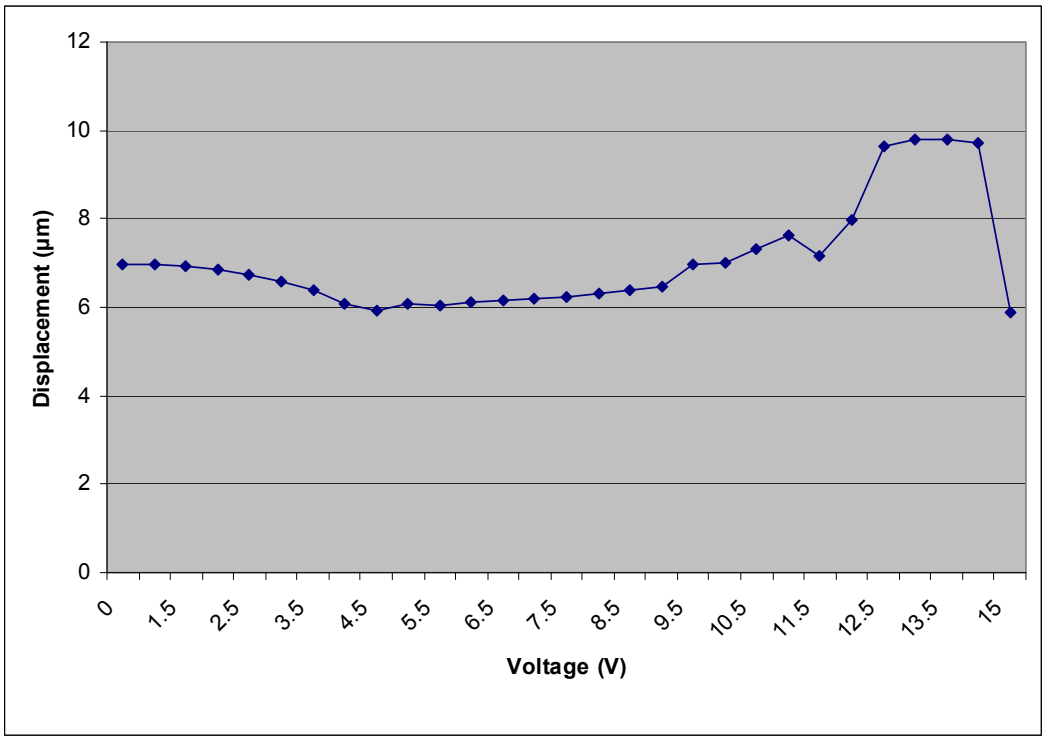


**Figure 31: Measured maximum vertical displacement in a vertical actuator.**

The cold arm appears to handle the majority of the heating instead of the hot arms, which means that the hot arms do not bend to create the desired deflection. This is due to the cold arm having a higher resistance than the hot arm due to the smaller cross-sectional area of thin parts of the cold arm, as shown in Figure 32 .

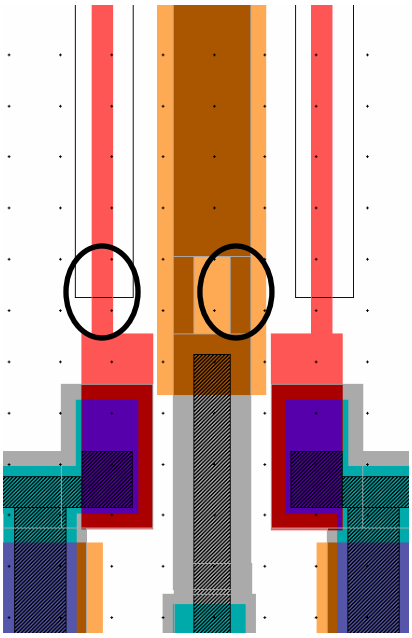

**Figure 32: Vertical actuator with circled hot and cold arm widths of 2 µm and 1.5 µm, respectively.**

These results indicate that in order to achieve an antenna perpendicular to the substrate, a lifting mechanism other than these vertical thermal actuators, such as residual stress cantilevers, must be used.

In an attempt to minimize the problem of joule heating in the cold arm, the gold wire connection between the hot arms was removed. Figure 33 shows the modified actuator where the gold was removed via a probe tip, and when compared with the actuator on the far left of the picture, one can see the missing connection.

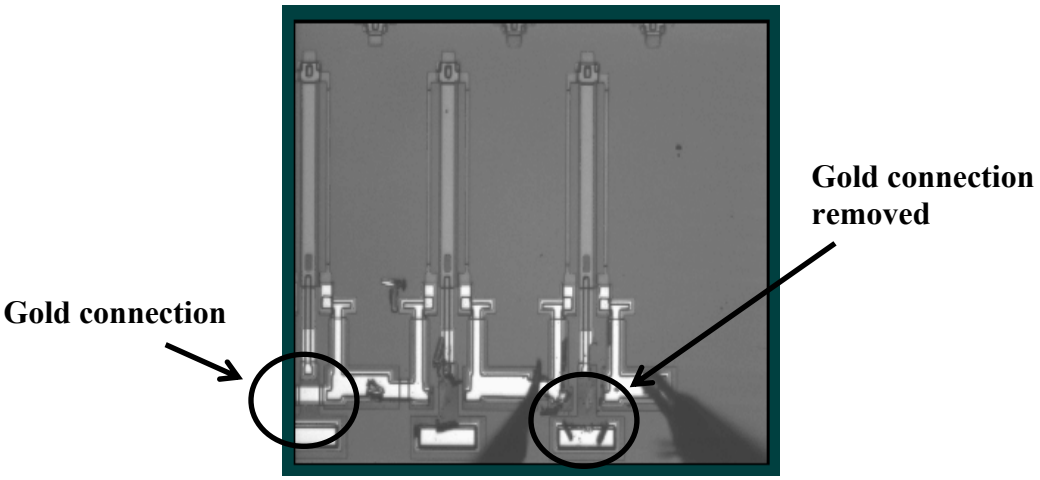


**Figure 33: Zygo picture of modified vertical actuator with circled missing gold connection on right and with an existing connection on the far left.**

When the modified actuator was tested, one hot arm was connected to power and the other to ground. The cold arm remained a floating node, yet still had deflection as it was attached to the hot arms at the end where displacement was to occur. The actuator's average deflection is shown in Figure 34.

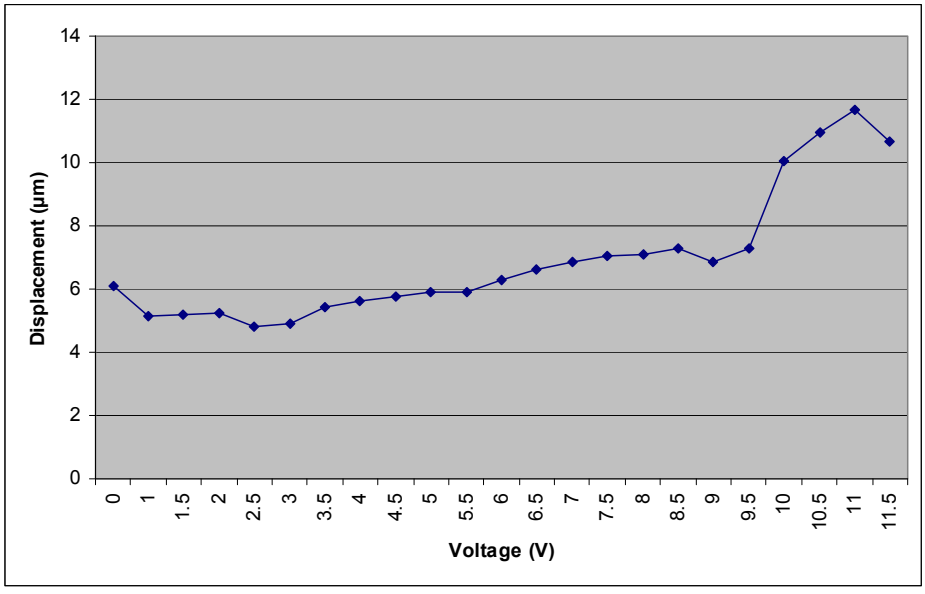


**Figure 34: Average maximum vertical displacement in a modified vertical actuator.**

### *Deployment Speed of Hinged Wheel Design*

To determine an approximate speed of deployment for an antenna from the hinged wheel design, an ideal frequency for operating a thermal actuator first needs to be discerned. In the first test, a 230 μm actuator was tested using a sinusoidal signal with a 2.5V amplitude and offset. The frequency was increased steadily up to 90 Hz. Once the 90 Hz signal was removed, the resulting position of the actuator was an additional 12 μm behind the original back-bent position of 4 μm behind the fabricated starting position. This massive deformation indicates that operating an actuator at such frequencies contributes to back-bending, likely because the hot arm does not have time to cool and return to its original position before the signal is again sent through it. The second round of testing involved an individual 257 μm Poly1 thermal actuator, which was tested with a sinusoidal signal with a 2.5 V amplitude and 2.5 V offset for 15 seconds at frequencies ranging from 1 to 60 Hz in increments of 1 Hz. The maximum deflection in the actuator decreased with increasing frequency, while the amount of back-bending increased because of inadequate cooling time for the hot arm. These results indicate that driving a thermal actuator bank at higher than approximately 30 Hz decreases the deflection the actuators are able to give as well as increases the chance of them deforming in such a manner as to prevent their usefulness.

Tests of the thermal actuator motors indicate that smaller teeth would be more beneficial. The distance the bank of actuators moves the translator is not necessarily enough to engage the teeth and move them. If there were 150 small teeth arrayed around the wheel approximately half the size of the current teeth, which are 30 μm tall and about

14 µm wide at the base, during each cycle the bank of actuators could move two teeth's worth of rotation, and if the banks were operated at 30 Hz, it would take approximately 2.5 seconds to deploy the 1mm antenna.

**Investigative Questions Answered**

The first design of the large wheel contained a short that precluded the operability of the large wheel design, as shown in Figure 35. This short was due to a gold pad providing a path between power and ground via the trench. One side of the gold pad touched the breached nitride on the perimeter of the chip, while the other side of the pad contacted the Poly0, Poly1, and Poly2 border of the trench that also connected to the Poly0 underneath the wheel. A positive voltage was applied to the Poly0 while ground was connected to the nitride breach elsewhere on the chip.

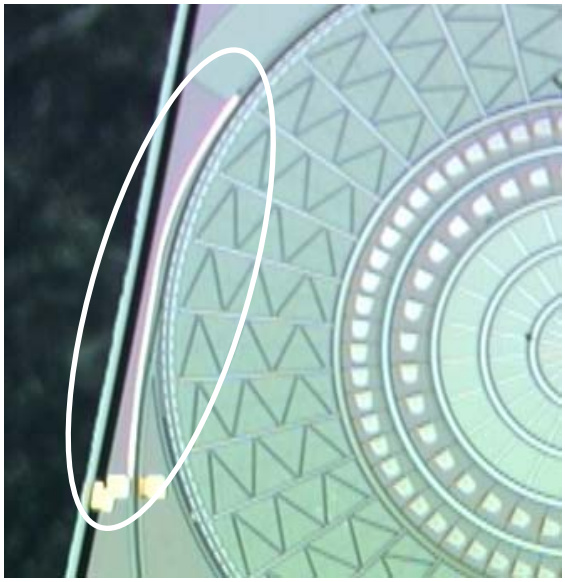

**Figure 35: Video screenshot of giant wheel with highlighted short**

The vertical thermal actuators when wired in series were not able to lift the 1mm long beam any measurable amount. However, the beam was lifted with microprobes and

successfully locked into place. Upon accidental destruction of the lock, the beam returned to its original position on the chip.

The two separate hinge designs each had problems too. Both hinges broke easily when the microprobe tips raised the flap. Upon closer inspection, it was found that the Poly2 layer had not been fully etched during the fabrication process, meaning the hinge was fused and not able to be moved. The amount of etching varied from chip to chip, as evidenced by the highlighted areas in Figure 36 and Figure 37.

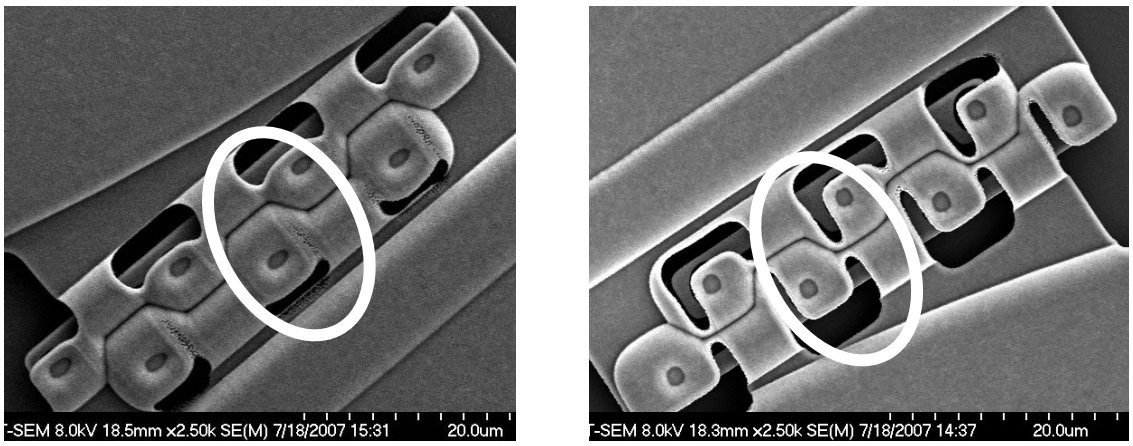


**Figure 36: SEM photo of hinge etching differences from two different chips.**

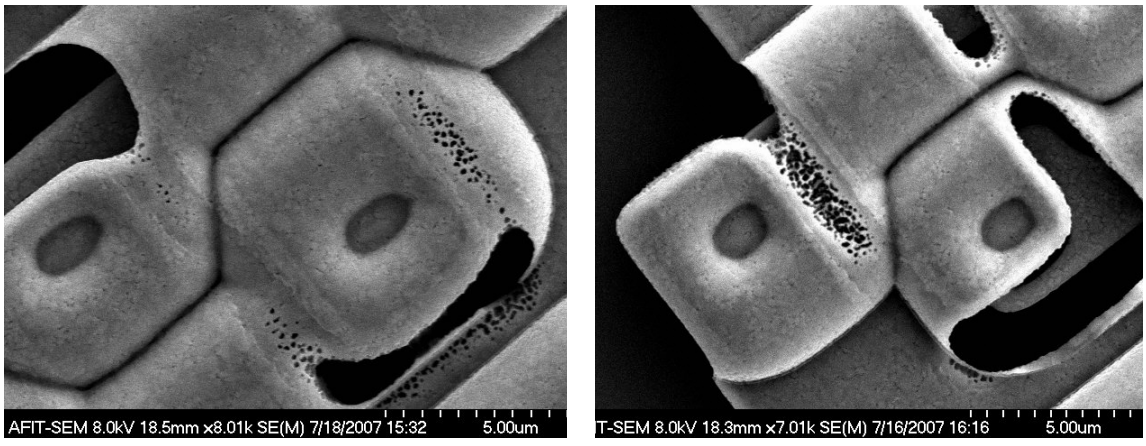


**Figure 37: Zoomed view of hinges in Figure 36.**

The residual stress cantilevers on the edges of the flaps of the hinged wheels prevented the edge of the flaps from touching the substrate in MUMPs run 78, as shown in Figure 38, but the hinges are again fused, preventing any flaps from standing up. Because of the fused hinges preventing upward movement, it is difficult to determine if the cantilevers were large enough to aid in self-assembly.

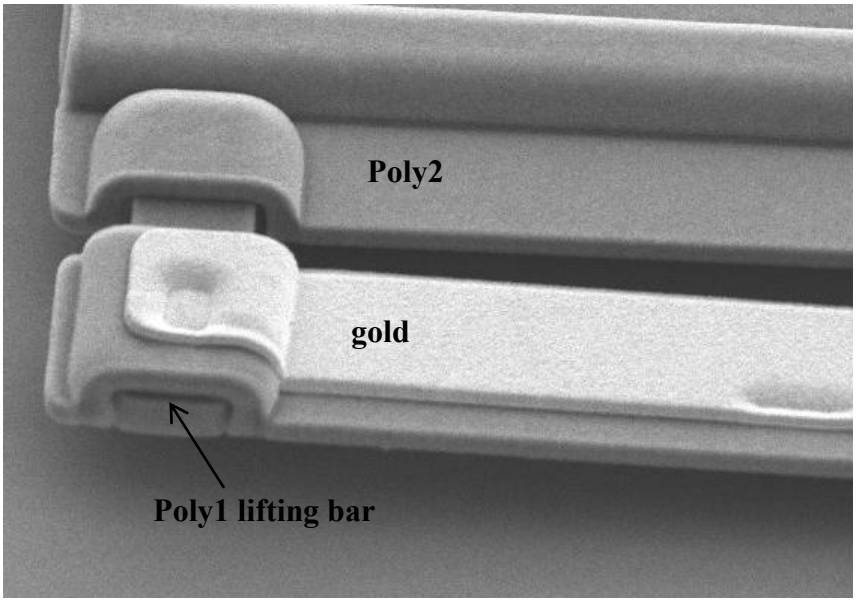


**Figure 38: SEM photo of residual stress cantilever and edge of slightly raised flap.**

Another fabrication difficulty encountered was the manufacturing of the pawl on the thermal actuator motors. In some instances, the head was not securely attached to the bar that was to push it, as shown in Figure 39. Despite this problem, systems that had a pawl still connected after release demonstrated that they would likely be able to work as designed if placed closer to the translator and wheel.

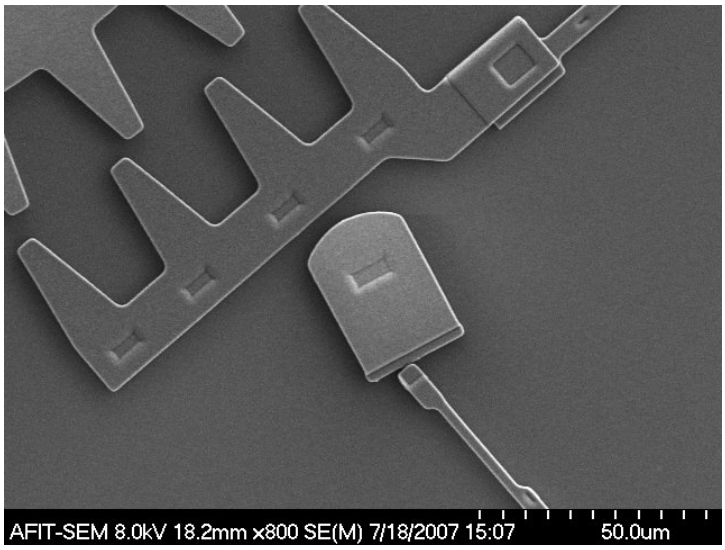


**Figure 39: SEM photo of broken pawl**

It was shown that both the vertical and horizontal actuators worked as intended, although the vertical actuator needed a slight modification, with the tips of each device showing displacement. However, the vertical actuators, as well as the residual stress cantilevers, create a raised portion of Poly2 on the antenna due to the conformal nature of the PolyMUMPs process that may preclude the antenna from easily sliding into the vertical position. As the vertical actuators are currently designed and arrayed, they will not lift the antenna enough for it to lock into place, as evidenced both by testing of the system and of individual actuators themselves.

In contrast, the residual stress cantilevers potentially can raise an antenna enough that the lock engages and it locks into place. If the antenna does not need to be exactly perpendicular to the substrate, slight modifications to the locking mechanism itself could allow the antenna to be completely self-assembling. Figure 40 shows two Poly2-gold cantilevers raising a Poly2 antenna.

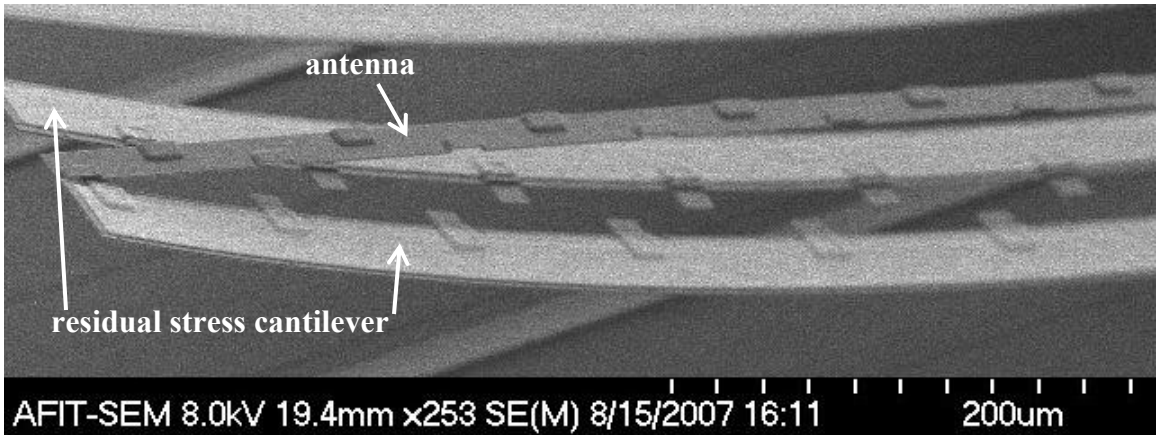


**Figure 40: SEM photo that shows residual stress Poly2-gold cantilevers raising a Poly2 antenna.**

One difficulty with this scheme of assembly stems from the ease with which a tab can hinder the assembly of the antenna instead of helping, as evidenced by Figure 41. In the figure, the cantilever on the right side is raising the antenna, while the one on the left is preventing the antenna from rising any higher than that cantilever's position. The tabs likely shifted to that hindering position during the releasing process. However, it must also be noted that one of the 1 mm antennas raised by residual stress cantilevers was locked into place after release without any human intervention. This stroke of luck was likely caused by movement of the antenna by one of the liquids during the releasing process or during the hot plate drying process. Unfortunately, this particular antenna cannot be retracted, as the mechanism implemented for retraction on the other vertical beam antennas was not included on this particular design.

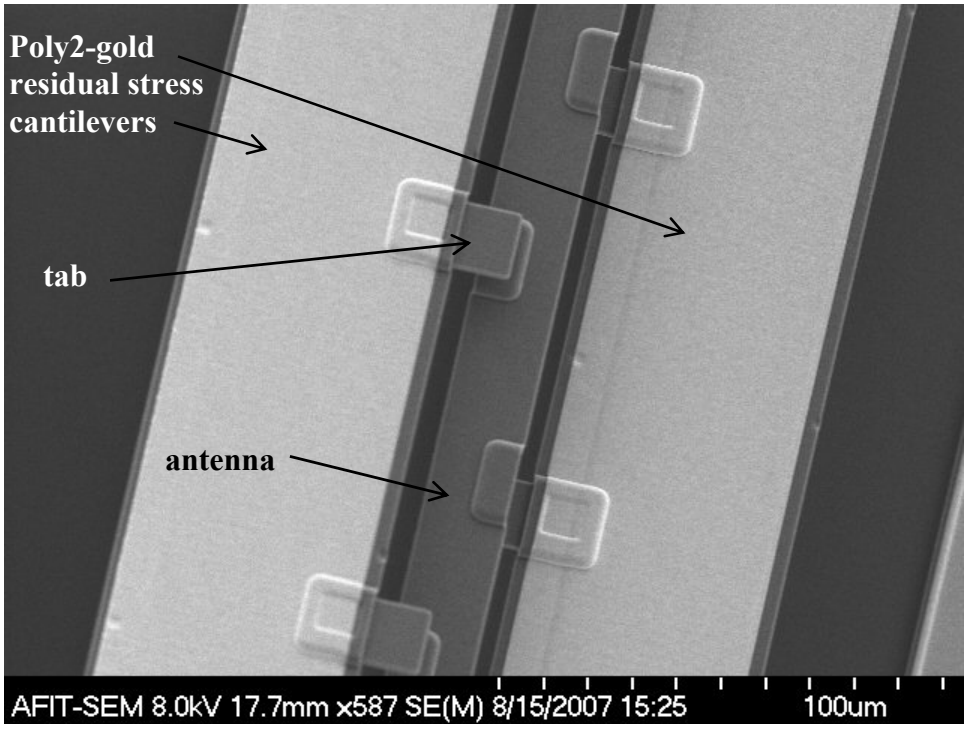


**Figure 41: SEM photo of Poly2-gold residual stress cantilevers counteracting each other by one preventing the antenna from moving into the proper position.**

The final variation of the vertical beam antenna was a simple 1 mm Poly2-gold cantilever, shown in Figure 42. The residual stress between the two layers was to serve as the only lifting mechanism and succeeded somewhat by slightly raising the antenna off the substrate. However, the internal stresses in the tip of the antenna caused the Poly2 layer to fracture in several places. This problem could be circumvented in future designs by corrugating the Poly2 layer underneath the gold so that the antenna can bend more easily.

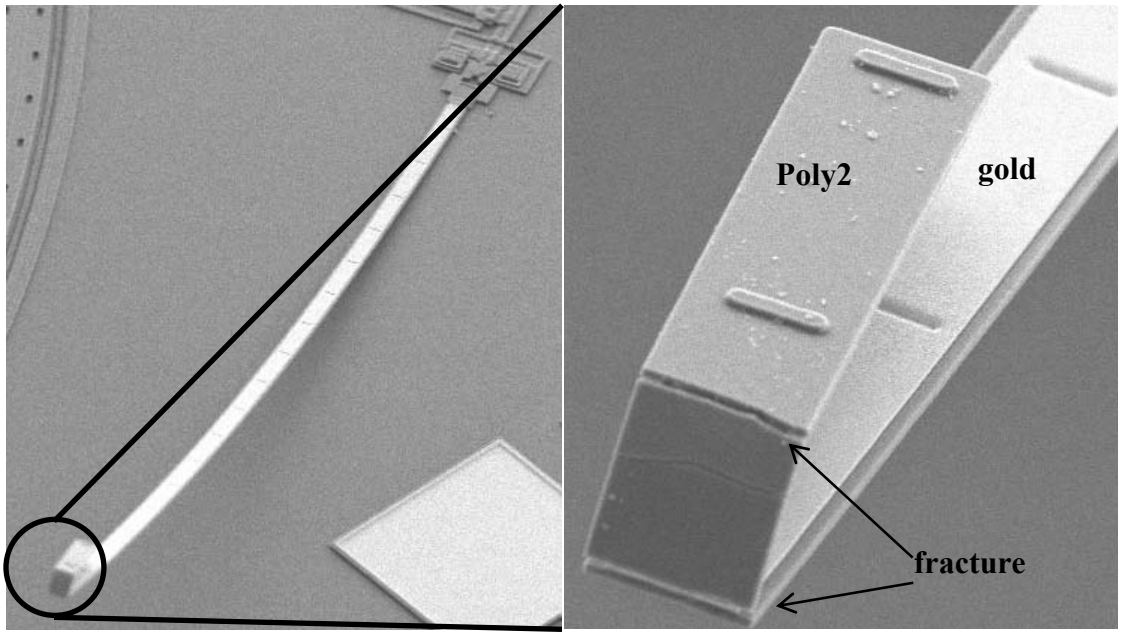


**Figure 42: SEM photo of residual stress 1 mm antenna with broken tip.**

**Summary**

This chapter detailed the successes and failures of each design that was able to be tested. The gears and beams design was unable to be successfully tested because it was so fragile that it easily broke after release. The residual stress cantilevers and thermal actuators were individually tested in order to characterize each of these devices. The 1 mm antenna that is raised perpendicular to the substrate had the most success. Although the antenna can be raised with microprobes, one antenna raised itself serendipitously into a locked position after release.

# V. Conclusions and Recommendations

## Conclusions of Research

The results of this research lead me to conclude that creating a MEMS device to deploy and retract an antenna is feasible. The most promising ideas include: 1) the hinged wheel, in which the antenna is wrapped around flaps perpendicular to a wheel that is turned by a bank of thermal actuators; 2) the design in which a set of gears translate the antenna on and off the substrate; and 3) the 1mm beam that locks into place perpendicular to the substrate. The first design needs slight modifications as well as potentially requiring an antenna other than a gold wire with a diameter of 10 μm. The second design merely requires slight modifications in order to obtain a working device to test, while the third design can be investigated more closely to find an optimal means of self-assembly.

Choosing those three designs as the most likely to succeed in future research does not preclude the feasibility of the other designs produced during this research. However, problems discovered with these other designs indicate that significant changes would likely need to be made in order for them to work.

## Significance of Research

The designs for a redeployment mechanism for an antenna investigated in this work are a step down the path of enabling humans to communicate with a hybrid insect or microrobot. From this proof-of-concept research, it can be concluded that it is feasible to enable a small antenna about the size of 1 mm to be deployed and retracted with

MEMS devices. The work is far from over, however; the mechanisms described in this document need to be further developed to have a higher reliability and become more robust.

**Recommendations for Action**

Neither hinged wheel design has proved unfeasible. The next generation of these devices should focus on creating a working hinge and then determining if the current placement of the lock or bondpads needs to be modified. Furthermore, the placement of the thermal actuator arrays and the engaging teeth size need to be adjusted so that the teeth on the gear can be engaged and moved. A result of this action will result in more teeth being required near the hinges in order for the wheel to spin, or the presence of a third and possibly fourth microengine so that teeth can be engaged at all times. A final area worth investigating is alternate engines comprised of either thermal actuators not meant to be plastically deformed or chevron actuators.

A redesign of the antenna translator would put the gears closer to each other, include staples to keep the antenna from moving in an undesired direction, and create a sturdier stop to prevent the antenna from being extended so far that it cannot be retracted. This design also has the potential to work well with another chip bonded on top, as a sturdier antenna and protection system could be created.

Finally, the vertical antenna needs a reliable assembly method. Although the residual stress cantilevers have worked, the current design is not reliable as it is fairly easy for the antenna to be jostled in such a manner so that the tabs on the cantilevers actually prevent the antenna from being raised any further. Perhaps the antenna does not

need to stand perpendicular to the substrate, in which case the cantilevers could work. Such a change would modify the resulting antenna pattern, potentially cutting the possible gain in half. If the angle at which the antenna stands needs to be adjusted, the lock must be modified to accommodate that change. Furthermore, it is necessary to develop a reliable method for retracting the antenna. Such a task could require only a repositioning of the vertical actuator.

**Recommendations for Future Research**

Future investigations down the path of developing a mechanism to retract and deploy an antenna should consider alternate motors, such as comb drives or a better application of the scratch drive. It would also be prudent to look at types of antennas other than a simple monopole. Perhaps another type of antenna would be more conducive for deploying and retracting and would be less susceptible to bending that is difficult to reverse.

Although the PolyMUMPs process allowed this research to be conducted at a relatively inexpensive cost of both time and money, another method of fabrication would benefit this research. The conformal nature, while at times a boon, was also a hindrance for some designs. Furthermore, the product developed was not as robust as it will eventually need to be.

Another idea for deploying an antenna could be tying that action to the movement of the insect's wings or some other physiological function. Coupling the two functions could save power and mass. Should the antenna be used not on a hybrid insect but a small robot, coupling the antenna movement with another robotic function such as

deploying the wings could also offer potential power or mass savings. Reliability and repeatability were not taken into account during this research effort, as deployment mechanisms were the main focus.

**Summary**

Although several designs did not completely work as intended, with minor modifications these mechanisms could be used as successful proof-of-concept devices to show the feasibility of creating such devices. This avenue of research is by no means exhausted and could have a significant impact on both the world of hybrid insects and microrobots.

## Appendix A: PolyMUMPs chip designs

Design 1: Miller1, PolyMUMPs run 75

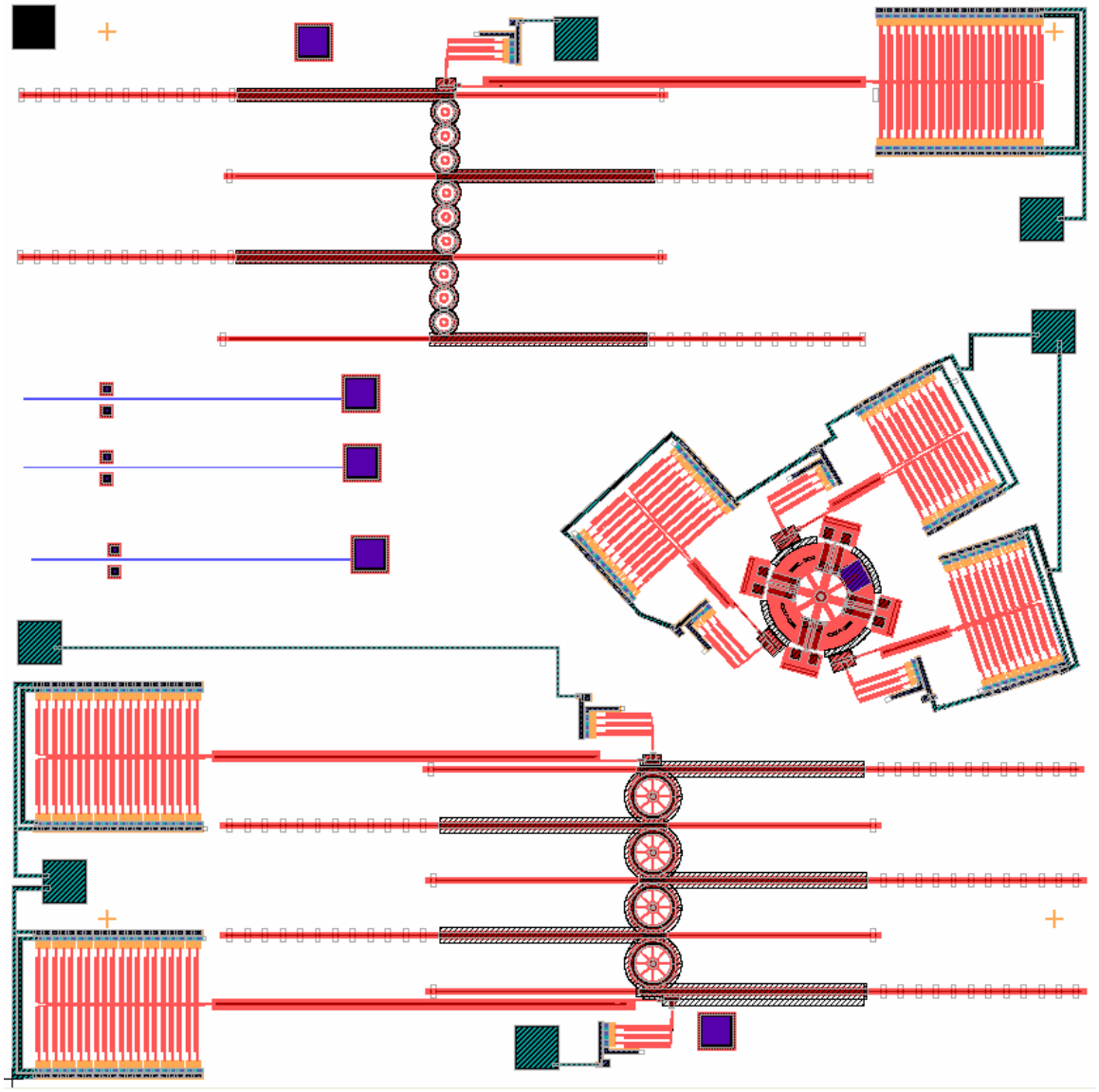

This chip tested two basic designs: the array of gears and beams and the hinged wheel. The former design had a large and small version. The wire is attached during a post-processing step and winds through posts on the end of each beam when in the retracted state. The thermal actuators move the beams so the posts are lined up as much as possible during the deployed state. The hinged wheel design is powered by thermal actuators also. The four flaps are raised perpendicular to the surface. The antenna is then wrapped around the wheel, rather like a water hose on a reel. The thin metal strips to the right of the hinged wheel serve as a test to see if it would be most practical to have the wire fabricated during the POLYMUMPS process.

Design 2:  Miller2, PolyMUMPs run 75

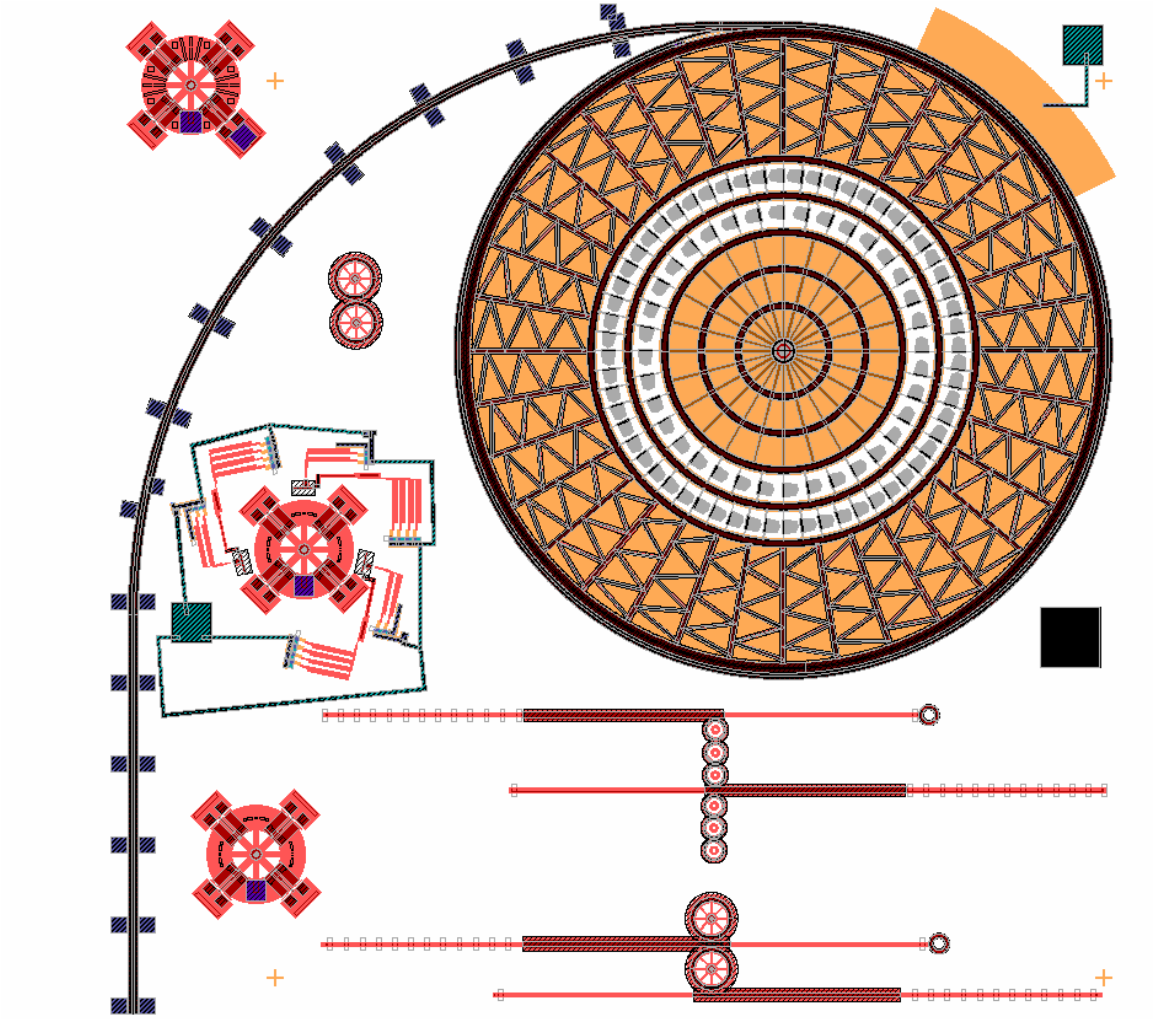

This chip tested a third idea of the large wheel, in addition to parts and variations of the first two designs.  The large wheel is powered by scratch drives.  The antenna is guided through the channel that comes off the side and should wind up neatly once around the wheel.  The two hinged wheels without any thermal actuators are for practicing lifting the flaps up.  One has an extra bonding place on a flap that lifts up; in this case, the feasibility of attaching the wire directly to the flap can be tested.  The third hinged wheel has a different arrangement of thermal actuators than that of the first design, and also has a smaller number for each section.  These differences in design can help determine if the other design is being over-powered.  Finally, the extra gears and beams were placed on here to see how easily they worked with each other.

Design 3: Miller2_round2, PolyMUMPs run 77

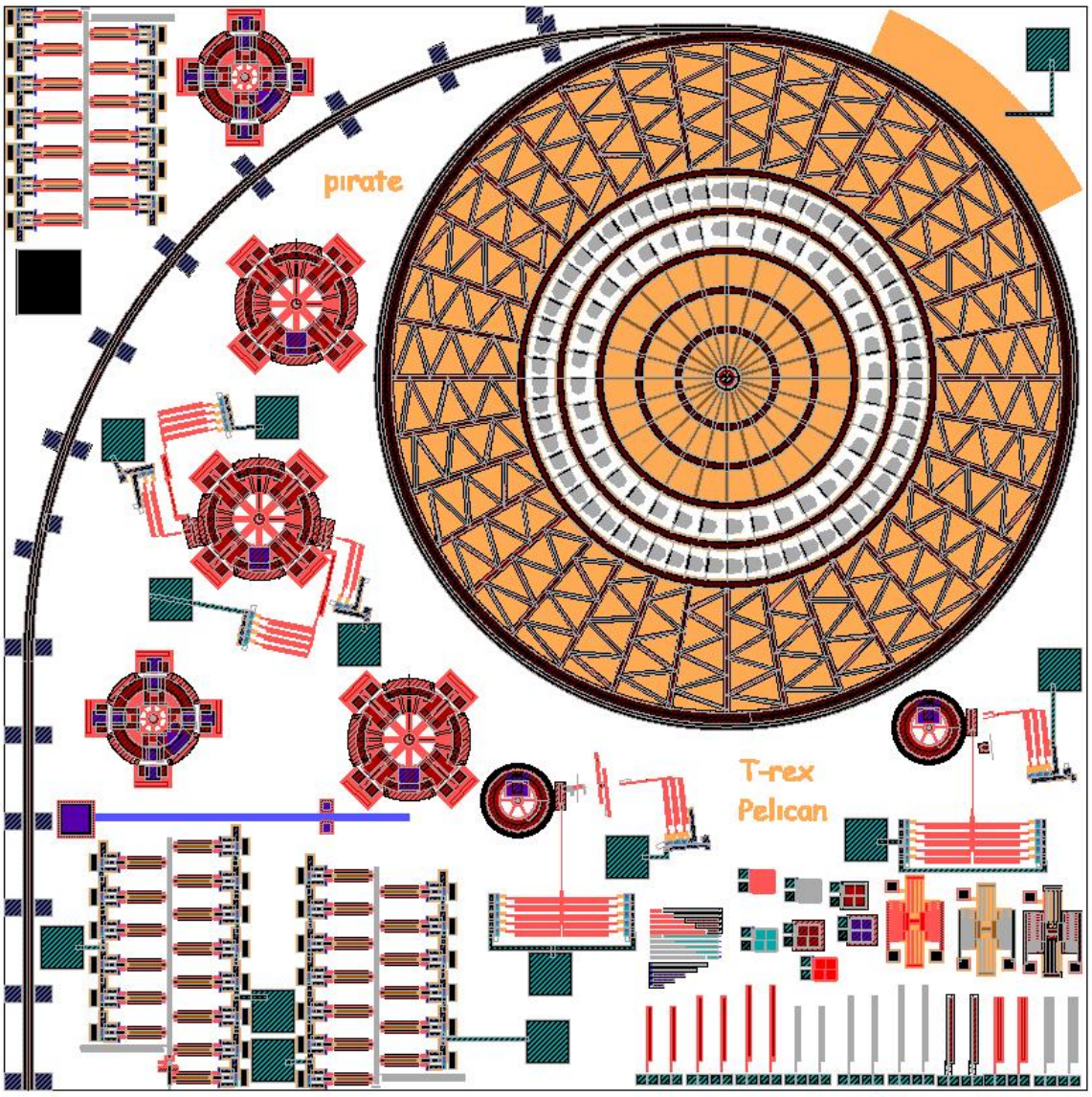


This chip contains the same large wheel found in Design 2, except that an anchor has been added to hold down the center of the wheel. The hinged wheel design has also had minor modifications to its locking mechanism to reduce potential complications in moving the flaps to a 90° position. A new hinged wheel design has been added, with the flaps to be self-assembled via solder balls. Another new design is that of the vertical beam antenna. There are two variants: both have a Poly2 spiral that will help pull the antenna back to the substrate, while one has a lock to hold the 1 mm beam in a vertical position from the other side of the hinge. Finally, the last new design was that of a wheel rotated by thermal actuators but with a groove around the outside for the wire. One variation has a pawl that must be moved across the chip. The other variation requires the pawl beam to be rotated 90°.

Design 4:  Miller3, PolyMUMPs run 77

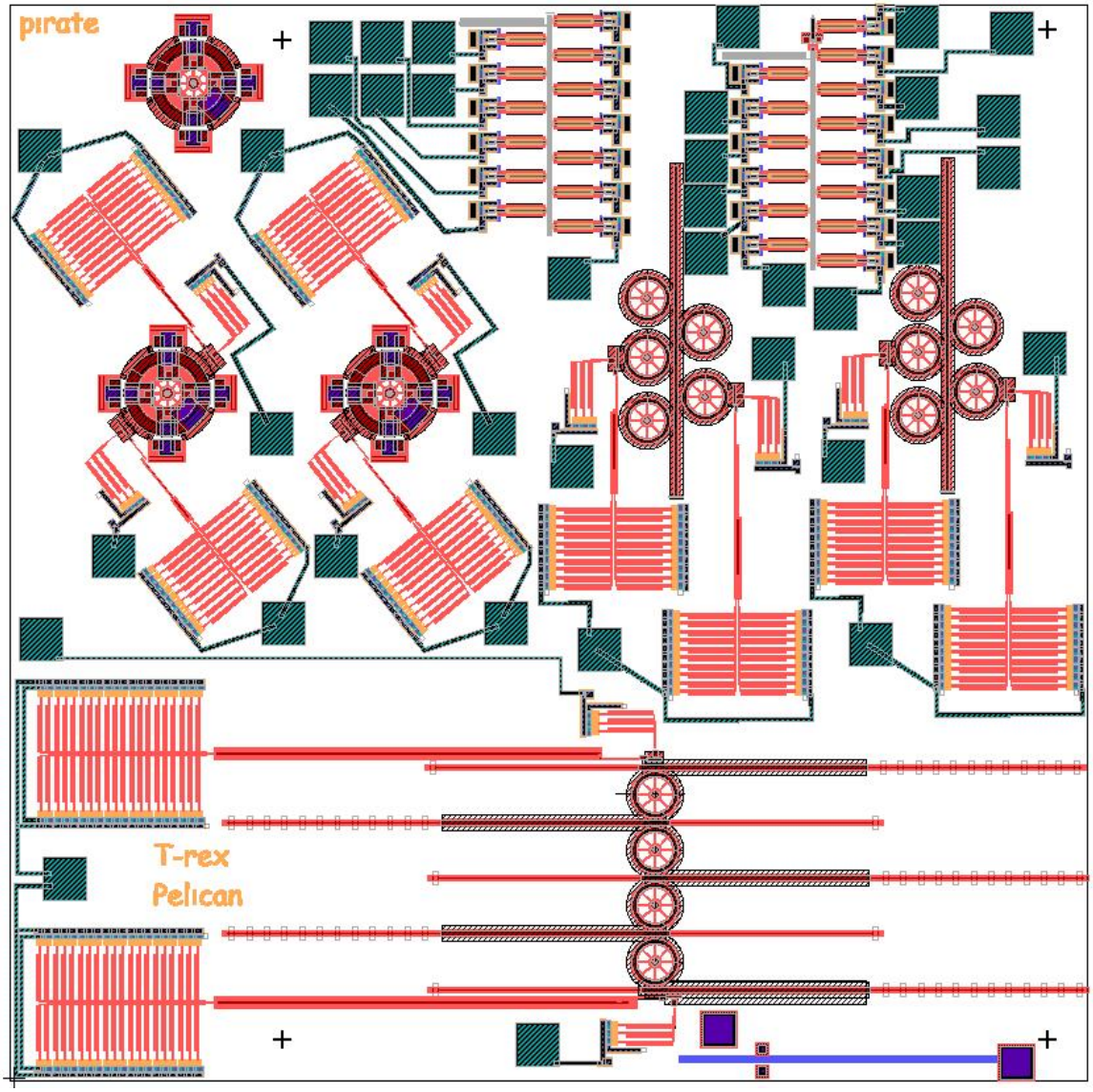


This chip has the new solder ball hinged wheel on the previous chip connected to a driving source.  It also contains both versions of the vertical beam antenna, which differ from those on the previous chip only in how they will be actuated.  On this chip, the vertical thermal actuators will be actuated in a cascaded manner, instead of all at the same time.  Finally, a new design of a simple beam that could extend off the chip has been introduced.

Design 5:  Miller4, PolyMUMPs run 78

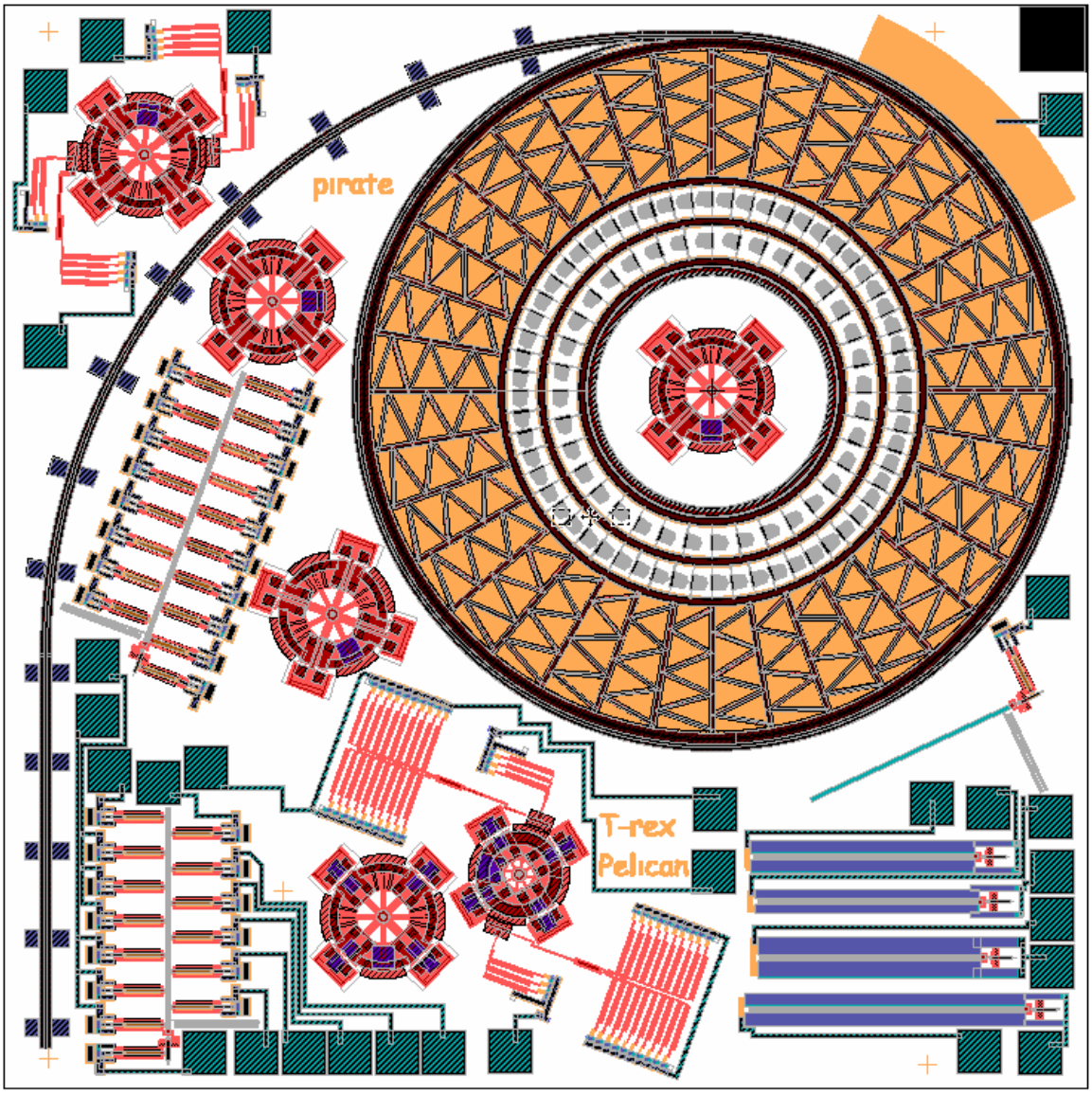


The large wheel had the area about which it rotates moved outward and was shrunk so that errors in alignment would be less likely to cause a short.  The hinged wheels had residual stress cantilevers added to each side of the flaps to aid in moving them to a vertical position.  Additionally, the locks on the flaps not meant for solder balls received a layer underneath so that they would be higher off the substrate than the plate and could move to lock the plate into position.  The vertical beam antenna that is to be moved into a position perpendicular to the chip also had residual stress cantilever beams added to the side to replace vertical thermal actuators and aid in self-assembly.  Finally, two vertical beam antennas with a length of 1.25mm were designed, one with the vertical thermal actuators and the other with the residual stress beams.

## Appendix B: Hybrid wheel design

The large wheel design was combined with the hinged wheel design to create a hybrid structure that would turn with a thermal actuator motor but would have the antenna coiled around it in a trench like the large wheel. The difficult part of this design is fabricating the trench and the teeth, pawl and translator required for motion at the same time. Because the PolyMUMPs process is conformal, the structures cannot be successfully created overlaying the trench. Two separate designs were envisioned to solve this problem. Figure 43 shows the first, which requires the beam that normally pushes the pawl to rotate 90° and lock into the pawl. The two pawl locks should slip over the teeth on the rotating beam to hold it in place.

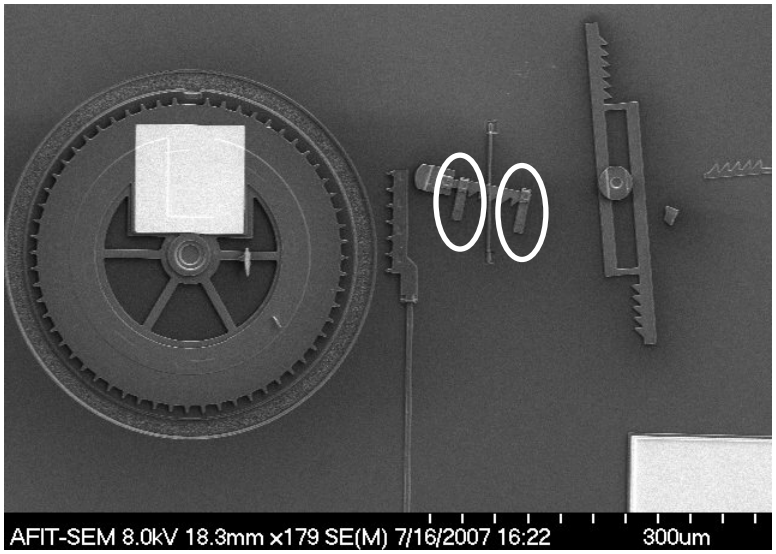


**Figure 43: SEM photo of combination wheel requiring rotation with circled pawl locks.**

The second design, shown in Figure 44, requires a micromanipulator to insert the pawl into its pushing beam. The pawl is secured by a thin Poly2 beam that can easily be broken. Both of these hybrid designs require some intricate assembly.

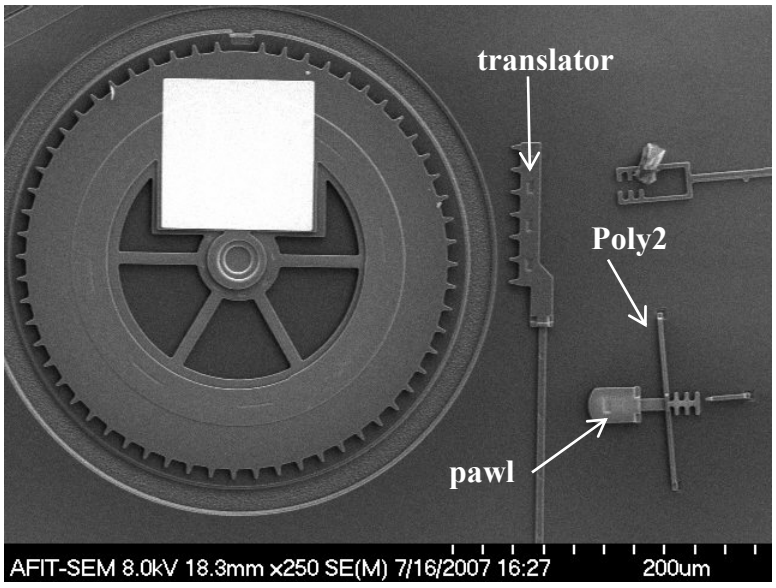


**Figure 44: SEM photo of combination Poly1-Poly2 stacked wheel requiring translation of pawl**

The design that required the arm of the pawl to rotate 90° does not work because of the conformal nature of the PolyMUMPs process. Figure 45 highlights the pin, made of Poly2, with lips on two sides. These lips do not allow the arm to turn.

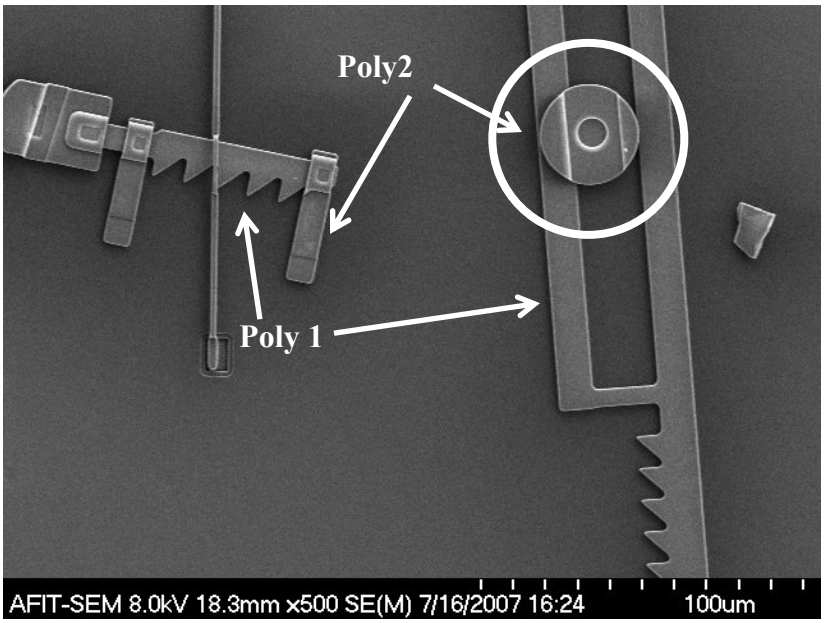


**Figure 45: SEM photo of pawl arm requiring rotation with circled pin**

## Bibliography

[1] Akiyama, T., D. Collard, and H. Fujita. "Scratch Drive Actuator with Mechanical Links for Self-Assembly of Three Dimensional MEMS," *Journal of Microelectromechanical Systems*, vol.6, pp10-17, 1997.

[2] Baglio, S., et al. "Technologies and Architectures for Autonomous "MEMS" Microrobots," *Proceedings of IEEE International Symposium on Circuits and Systems*, vol. 2, pp584–587, 2002.

[3] Bozkurt, A, et al. "Microprobe Microsystem Platform Inserted During Early Metamorphosis to Actuate Insect Flight Muscle," IEEE International Conference on MEMS, pp 405-408, 2007.

[4] Butler, T. J., V. M. Bright, and W. D. Cowan. "Average Power Control and Positioning of Polysilicon Thermal Actuators," *Sensors and Actuators, vol,* 72, pp88–97, 1999.

[5] Cetiner, B. A., et al. "Integrated MEM Antenna System for Wireless Communications," Microwave Symposium Digest, p1333-1336, 2002.

[6] Chiao, J. C. et al. "MEMS Millimeterwave Components," Microwave Symposium Digest, p463-466, 1999.

[7] Comtois, J. H. and V. M. Bright. "Applications for Surface-Micromachined Polysilicon Thermal Actuators and Arrays," *Sensors and Actuators*, vol. 58, pp19-25, 1997.

[8] Donald, B., et al. "An Untethered, Electrostatic, Globally Controllable MEMS Micro-Robot," *Journal of Microelectromechanical Systems*, vol. 15, pp1-15, Feb 2006.

[9] Ebefors, T., E. Kälvesten, and G. Stemme. "New Small Radius Joints Based on Thermal Shrinkage of Polyimide in V-grooves for Robust Self-Assembly 3D Microstructures," *Journal of Micromechanics and Microengineering*, vol. 8, pp. 188–194, 1988.

[10] Fan, L., M.C. Wu, and K.D. Choquette. "Self Assembled Micro-Actuated XYZ Stages for Optical Scanning and Alignment," International Conference on Solid-State Sensors and Actuators, pp319-322, 1997.

[11] Harsh, K. F., V.M. Bright, and Y.C. Lee. "Solder Self- Assembly for Three-Dimensional Microelectromechanical Systems," *Sensors and Actuators A: Physical,* vol. 77, pp237-244, 1999.

[12] Johnstone, R. W. and M. Parameswaran. "Modelling Surface-Micromachined Electrothermal Actuators," *Canadian Journal of Electrical and Computer Engineering*, vol. 29, pp193-202, July 2004.

[13] Kolesar, E, et al. "Design and Performance of an Electrothermal MEMS Microengine Capable of Bi-Directional Motion," *Thin Solid Films,* vol. 447-448, pp481-488, 2004.

[14] Kolesar, E, et al. "Precision Bi-directional Motion of a Linear Mechanical Shuttle with an Electrothermal Microengine," *Thin Solid Films,* vol. 469-470, pp450-454, 2004.

[15] Lal, Amit. "Proposer Information Pamphlet." 9 Mar 2006. DARPA MTO. 31 Mar 07. <http://www.darpa.mil/mto/solicitations/baa06-22/doc/pip.doc>.

[16] Lal, Amit. "Hybrid Insect MEMS Proposer's Day." 24 Mar 2006. DARPA MTO. 31 Mar 07. <http://www.darpa.mil/mto/solicitations/baa06-22/pdf/lal_proposerday.pdf>.

[17] Lam, K., E Johnson and L. Lin. "A Bio-Solar Cell Powered by Sub-Cellular Plant Photosystems," IEEE International Conference on MEMS. 2004.

[18] Lam, K. , M. Chiao and L. Lin. "A Micro Photosynthetic Electrochemical Cell" IEEE International Conference on MEMS. 2003.

[19] Miura, H., et al. "Insect-Model Based Microrobot," *Transducers*, pp. 392–395, Jun. 1995.

[20] Paul, A., et al. "Surgically Implanted Micro-Platforms in *Manduca Sexta* Moths," Solid State Sensor and Actuator Workshop, pp209-211, 2006.

[21] PolyMUMPs Design Handbook Revision 11.0 < http://www.memscap.com/mumps/documents/PolyMUMPs.DR.v11.pdf>. 2005.

[22] Que, L., J.-S. Parl, and Y. B. Gianchandani. "Bent-beam Electro-thermal Actuators for High Force Applications," IEEE International Conference on MEMS, pp31-36, 1999.

[23] Reid, J. R., V. M. Bright, and J. H. Comtois. "Automated Assembly of Flip-Up Micromirrors," *Transducers*, pp347-350, 1997.

[24] Shimoyama, I., O. Kano, and H. Miura. "3D Microstructures Folded by Lorentz Force," *11th International Workshop on Microelectromechanical Systems Proceedings*, pp. 24–28, 1998.

[25] Smela, E., O. Inganä, and I. Lundströ. “Self-Opening and Closing Boxes and Other Micromachined Folding Structures,” *International Conference on Solid-State Sensors and Actuators Proceedings*, pp. 350–351, 1995.

[26] Syms, R. R. A. and E. M. Yeatman. “Self-Assembly of Fully Three-Dimensional Micro-Structures Using Rotation by Surface Tension Forces,” *Electronics Letters*, vol. 29, pp. 662–664, 1993.

[27] Syms, R.R.A. “Self-Assembled 3-D Silicon Microscanners with Self-Assembled Electrostatic Drives,” *IEEE Photonics Technology Letters,* vol. 12, pp1519-1521. 2000.

[28] Tuck, K. et al. “A Study of Creep in Polysilicon MEMS Devices,” *Journal of Engineering Materials and Technology*, vol. 127, pp90-96, 2005.

[29] Yan D., A. Khajepour, and R. Mansour. “Design and Modeling of a MEMS Bidirectional Vertical Thermal Transducer,” *Journal of Micromechanics and Microengineering*, vol. 14, pp841–850, 2004.

[30] Yoon, Y., et al. "Surface Micromachined Electromagnetically Radiating RF MEMS," Solid-State Sensor, Actuator, and Microsystems Workshop Digest, pp. 328-331, 2004.

[31] Yoon, Y., et al. “A Vertical W-band Surface-Micromachined Yagi-Uda Antenna”, *2005 IEEE-APS/URSI Symposium Proceedings*, 2005.

[32] Yoon, Y., et al. “Surface-Micromachined Millimeter-Wave Antennas.” International Conference on Solid-State Sensors, Actuators, and Microsystems, vol. 1, pp1986-1989, 2005.

## Vita

Virginia Miller was born in 1984 in Winston-Salem, NC. She lived in the nearby town of Pfafftown until her family moved to Bonn, Germany in 2000. While in Bonn, she, her brother and little sister made the most of their time in a foreign culture, making friends from all over the world. She and her brother joined a local swim team, SSF Bonn, where they were able to relate with another culture through swimming. A year and half later, her family returned to Winston-Salem, where she graduated from Reynolds High School in 2002. Ginny then received an appointment to the US Air Force Academy, where she swam with the Division I swim team. She graduated from Cadet Squadron 15 with a degree in electrical engineering on May 31, 2006 and was commissioned as a 2nd Lieutenant in the US Air Force. She started at the Air Force Institute of Technology in the fall of 2006, where she studied MEMS and microelectronics. Upon graduation from AFIT, she will work in the Sensors Directorate of the Air Force Research Laboratory at Wright-Patterson AFB, OH.

# REPORT DOCUMENTATION PAGE

*Form Approved*
*OMB No. 074-0188*



| 1. REPORT DATE *(DD-MM-YYYY)* | 2. REPORT TYPE | 3. DATES COVERED *(From – To)* |
|---|---|---|
| 13-09-2007 | Master's Thesis | Sept 2006 – Sept 2007 |

**TITLE AND SUBTITLE**

CONCEPTUAL MEMS DEVICES FOR A REDEPLOYABLE ANTENNA

**5a. CONTRACT NUMBER**

**5b. GRANT NUMBER**

**5c. PROGRAM ELEMENT NUMBER**

**AUTHOR(S)**

Miller, Virginia, 2nd Lieutenant, USAF

**5d. PROJECT NUMBER**

**5e. TASK NUMBER**

**5f. WORK UNIT NUMBER**

**7. PERFORMING ORGANIZATION NAMES(S) AND ADDRESS(S)**

Air Force Institute of Technology
Graduate School of Engineering and Management (AFIT/EN)
2950 Hobson Way, Building 640
WPAFB OH 45433-8865

**8. PERFORMING ORGANIZATION REPORT NUMBER**

AFIT/GE/ENG/07-30

**9. SPONSORING/MONITORING AGENCY NAME(S) AND ADDRESS(ES)**

Jason Foley, AFRL/MNMF
306 W. Eglin Blvd, Bldg 432
Eglin AFB, FL 32542
(850) 833-0584 jason.foley@eglin.af.mil

**10. SPONSOR/MONITOR'S ACRONYM(S)**

**11. SPONSOR/MONITOR'S REPORT NUMBER(S)**

**12. DISTRIBUTION/AVAILABILITY STATEMENT**

APPROVED FOR PUBLIC RELEASE; DISTRIBUTION UNLIMITED.

**13. SUPPLEMENTARY NOTES**

**14. ABSTRACT**

Micro-Electro-Mechanical Systems (MEMS) are becoming an integral part of our lives through a wide range of applications, including MEMS accelerators for air bag deployment in vehicles, micromirrors in projection devices, and various sensors for chemical/biological applications. MEMS are a key aspect of ever-increasing significance in a myriad of commercial and military applications. Because of this importance, this thesis utilizes MEMS devices that can deploy and retract an antenna suitably sized for placement on an insect or microrobot for communication purposes. A target monopole antenna with a length of 1 mm was used as a test metric. From this requirement, several MEMS designs using scratch drives and thermal actuators as the basis for powering the motor were developed. Some of the fabricated and tested designs included a gear with side flaps that flip up perpendicular to the substrate; gears that push an antenna beam off the edge of the substrate; and an antenna beam that is moved upwards such that it stands perpendicular to the substrate. These designs had the highest likelihood of success. Other designs included an array of micro gears and guiding beams, a large wheel powered by scratch drives, and a gear with the pawl requiring assembly. For these designs to be successful, several basic modifications would be necessary. The antenna beam that moves into a position perpendicular to the substrate was successfully self-assembled.

**15. SUBJECT TERMS**

MEMS, antenna, PolyMUMPs, insect

| 16. SECURITY CLASSIFICATION OF: | | | 17. LIMITATION OF ABSTRACT | 18. NUMBER OF PAGES | 19a. NAME OF RESPONSIBLE PERSON |
|---|---|---|---|---|---|
| a. REPORT | b. ABSTRACT | c. THIS PAGE | | | LaVern A. Starman, Maj, USAF (ENG) |
| U | U | U | UU | 82 | 19b. TELEPHONE NUMBER *(Include area code)* (937) 255-3636, ext 4618 (LaVern.Starman@afit.edu) |